

Models of Rapidly Rotating Neutron Stars

By
Paschalidis Vasileios

Supervisors
K. Kokkotas, N. Stergioulas

Aristotle University of Thessaloniki
Department of Physics

July 2003

Acknowledgements

At this point, I would like to thank my professor K. Kokkotas for helping me both in technical and physical issues related to this project, as well as for the opportunity to expand my horizons on both Astrophysics and computers. I am also required to say a great thanks to my professor N. Stergioulas for every elucidating conversation we had, as well as for every piece of advice he gave me while I was working on my diploma thesis. Undoubtedly, this work would not have its current character and quality without his valuable guidance. Finally, I thank with all my heart, my parents for their invaluable support and encouragement.

Abstract

The diploma thesis in hand is a Newtonian approach to the description of the basic properties of rapidly rotating Neutron Stars. We begin with a brief reference to the history of the observational and theoretical study of stellar rotation as a whole. Thereinafter, by making use of mechanics of continuum media and more specifically fluid mechanics, we gradually present the modern Newtonian theory of rotating stars. The most important parts of this work are the third one, where a variant of the Self-Consistent Field method developed by Izumi Hachisu (abbreviated by HSCF) is introduced, and the fourth one, where we set out the numerical results produced by the simulation of several models of rapidly rotating Neutron Stars.

Contents

1	An Historical Overview	5
1.1	Discovery of the Solar Rotation	5
1.2	Early Measurements of Stellar Rotation	6
1.3	Rotating Fluid Masses	8
1.4	The Golden Age of Stellar Rotation	10
2	Permanent Rotations	12
2.1	Introduction	12
2.2	Assumptions and Definitions	12
2.3	Barotropes, Pseudo-Barotropes and Baroclines	15
2.4	Spheroidal Stratifications	18
2.5	Some Inequalities	19
2.6	The Outer Gravitational Field	23
2.7	Integral of Motion	24
3	Stellar Models - Techniques	26
3.1	The Self-Consistent Field Method (SCF)	26
3.2	The HSCF Method	28
3.2.1	Formulation of Basic Equations and Assumptions.	29
3.2.2	Plan of the Method	31
3.2.3	Numerical Technique	37
4	Numerical Results	42
4.1	Rigidly Rotating Neutron Stars	42
4.2	Differentially Rotating Polytropes	46
4.3	Extensions of the HSCF Method	49
A	APPENDIX	50
A.1	A Few Words on Legendre Polynomials	50
B	APPENDIX	55
B.1	Stationary Newtonian Star	55
B.2	Numerical Solution	56
C	APPENDIX	59
C.1	Program for the HSCF Method	59

Models of Rapidly Rotating Neutron Stars

Paschalidis Vasileios

28th August 2003

1 An Historical Overview

1.1 Discovery of the Solar Rotation

The study of stellar rotation began about the year 1610, when sunspots were observed for the first time through a refracting telescope. The first public announcement of an observation came in June 1611 from Johannes Goldschmidt (1587-1615)– a native of East Friesland, Germany – who is generally known by his Latinized name Fabricius. From his observations he correctly inferred the spots to be parts of the sun itself, thus proving axial rotation. He does not appear to have appreciated the importance of his conclusion, and pursued the matter no further.

According to his own statement, Galileo Galilei (1564-1642) observed the sunspots toward the end of 1610. He made no formal announcement of the discovery until May 1612, by which time such observations had also been made by Thomas Harriot (1560-1621) in England and by the Jesuit Father Christoph Scheiner (1575-1650) in Germany. A controversy about the nature of sunspots made Scheiner a bitter enemy of Galileo and developed into a quarrel regarding their respective claims to discovery. Since Scheiner had been warned by his ecclesiastical superiors not to believe in the reality of sunspots (because Aristotle’s works did not mention it), he announced his discovery in three letters written under the pseudonym of Apelles. He explained the spots as being small planets revolving around the Sun and appearing as dark objects whenever they passed between the Sun and the Observer. These views opposed those of Fabricius and Galileo, who claimed that the spots must be on or close to the solar surface.

In the following year, 1613, Galileo replied with the publication of his *Istoria e Dimostrazioni intorno alle Macchie Solari e loro Accidenti*. In these three letters he refuted Scheiner’s conclusion and, for the first time, publicly declared his adherence to the heliocentric theory of the solar system – thus initiating the whole sad episode of his clashes with the Roman Inquisition. As far as solar rotation is concerned, one of his arguments is so simple – and at the same time so convincing – that it may be worthwhile to reproduce it here. Galileo noticed that a sunspot took about fourteen days to cross the solar disk, and that this time was the same whether the spot passed through the center of the solar disk or along a shorter path at some distance from the center. However, he also noticed that the rate of motion of a spot was by no means uniform, but that the motion always appeared much slower when near the solar limb than when near the center. This he recognized as an effect of foreshortening, which would result if and only if the spots were near the solar surface.

Scheiner’s views were thus crushingly refuted by Galileo. Eventually, the Jesuit Father’s own observations led him to realize that the Sun rotates with an apparent period of about 27 days. To him also belongs the credit of determining with considerably more accuracy than Galileo the position of the Sun’s equatorial plane and the duration of its rotation. In particular, he showed

that different sunspots gave different periods of rotation and, furthermore, that the spots farther from the solar equator moved with a slower velocity. Scheiner published his collected observations in 1630 in a volume entitled *Rosa Ursina sive Sol*. This was truly the first monograph on solar physics.

For more than two centuries the problem of solar rotation was practically ignored, and it is not until the 1850s that any significant advance was made. Then, a long series of observations of the apparent motion of sunspots was undertaken by Richard Carrington (1826-1875), a wealthy English amateur, and by Gustav Spörer (1822-1895), a German astronomer. They both confirmed, independently, that the outer visible envelope of the Sun does not rotate like a solid body, i.e., its period of rotation varies as a function of heliocentric latitude. They showed that the rotation period is minimum at the equator and increases gradually toward the poles. After correcting for the annual motion of the earth around the Sun, Carrington derived a mean period of 24.96 days at the solar equator.

Several attempts have been made to represent analytically the dependence of rotational speed on latitude by means of an empirical formula. From his own observations made during the period 1853-1861, Carrington derived the following expression for the daily angle of solar rotation:

$$\xi(\text{deg/day}) = 14^\circ.42 - 2^\circ.75 \sin^{7/4} \phi, \quad (1)$$

where ϕ is the heliocentric latitude. Somewhat later, the French astronomer Hervé Faye (1814-1902) found that the formula

$$\xi(\text{deg/day}) = 14^\circ.37 - 3^\circ.10 \sin^2 \phi \quad (2)$$

more satisfactorily represented the dependence of rotation on heliocentric latitude. Other formulae have been suggested, but Faye's empirical law has remained in use until now.

The next step was taken by Hermann Vogel (1841-1907) in Potsdam. In 1871, by means of a new spectroscope devised by Johann Zöllner (1834-1882), Vogel showed that the solar rotation can be detected from the relative Doppler shift of the spectral lines at opposite edges of the solar disk, one of which is approaching and the other is receding.¹ Accurate and extensive observations were made by Nils Dunér (1839-1914) in Lund and Upsala, and then by Jacob Halm (1866-1944) in Edinburgh. Dunér and Halm used a relative method of measurement based on the difference in behavior of the solar and terrestrial lines. They concluded that Faye's law could adequately represent the spectroscopic observations also, but their coverage of latitude was double that of the sunspot measurements. After these early visual observations made during the period 1887-1906, photography almost completely superseded the human eye. The first spectrographic determinations of solar rotation were undertaken at the turn of the century by Walter S. Adams (1876-1956) and George E. Hale (1868-1938) at Mount Wilson Solar Observatory, California.

1.2 Early Measurements of Stellar Rotation

In 1877, Sir William de Wiveleslie Abney (1843-1820) suggested that axial rotation might be responsible for the great widths of certain stellar absorption lines. He correctly pointed out that a spectrum is actually a composite of light from all portions of the star's disc. Because of Doppler effect, wavelengths in the light of the receding edge of the star would be shifted

¹In 1848 the French physicist Armand-Hippolyte Fizeau showed that stellar radial velocities are much too small to cause an appreciable color change, but that the Doppler effect could be detected by very small changes in the wavelengths of individual spectral lines. The experiment was successfully performed for the first time in 1868 by Sir William Huggins (1824-1910), who was able to measure the minute Doppler shifts of the hydrogen lines in the spectrum of Sirius.

toward the red, while those from the approaching edge would be shifted toward the violet. Abney concluded: " There would be a total broadening of the line, consisting of a sort of double penumbra and a black nucleus More than this, rotation might account for the disappearance of some of the finer lines of the spectrum. . . . I'm convinced that from a good photograph much might be determined" (M.N. 37, 278, 1877). These suggestions were severely criticized by Vogel because some of the stellar spectra contained both broad and narrow lines. Concerning the use of photography, Vogel went further in saying that "even on the most successful photograph only relative measures of lines would be possible in regard to rotation; the widths of lines on different photographic plates would depend upon the length of exposure, the sensitivity of the plate and the length of development" (A.N. 90, 71, 1877).

Abney's suggestion found little favor among his contemporaries. The reason may be due to the enormous weight accorded the opinion of Vogel, who, for many years, dominated the field of stellar spectroscopy. In any case, only a few years after his emphatic predictions, Vogel introduced photography into stellar spectroscopy and completely reversed his stand in 1898, expressing himself in favor of the hypothesis that rotation does produce a measurable broadening of stellar lines.

As often happens in the history of science, the discovery of axial rotation in stars was purely accidental. In 1909, convincing evidence of rotation in the eclipsing and spectroscopic binary δ Librae was obtained by Frank Schlesinger (1871-1943), then at Allegheny Observatory, Pittsburgh. He noticed that just before and just after light minimum, the radial velocities he had measured on his spectrograms departed from their expected values. A positive excess was observed just before mid-eclipse, while after mid-eclipse the departure was found to be negative. Schlesinger concluded that this occurrence could be produced if the brightest star rotates around an axis, so that, at the time of partial eclipse, the remaining portion of its apparent disc is not symmetrical with respect to its axis of rotation. One year later, Schlesinger observed a similar phenomenon in the eclipsing system λ Tauri. In 1924, at the University of Michigan, Richard A. Rossister (1886-1977) positively established the effect in β Lyrae and gave a complete curve of the residuals in velocity during the eclipse, while Dean B. MacLaughlin (1901-1965) investigated the effect in the binary star β Persei. These were the first accurate measurements of the axial rotation of stars.

Another approach to the determination of stellar rotation was provided by spectroscopic binaries not known to be variable in light. In 1919, at Mount Wilson, Adams and Alfred H. Joy (1882-1973) studied the binary W Ursae Majoris of spectral type F8 and having a period of 0.334 day. They observed that "the unusual character of the spectral lines is due partly to the rapid change in velocity during even our shortest exposures but mainly to the rotational effect in each star, which may cause a difference of velocity in the line of sight of as much as 240 *km/sec* between the two limbs of the star" (Ap.J. 49, 190, 1919). Ten years later, a systematic study of rotational line-broadening in spectroscopic binaries was undertaken jointly by Grigori Abramovich Shajn (1892-1956) in the former Soviet Union and Otto Struve (1897-1963) in the United States (their collaboration took place by mail). Shajn and Struve positively established that in spectroscopic binaries of short period, at least, line broadening is essentially a result of rotation.

The next step was to extend these measurements to single stars. Indeed, the possibility existed that rapid rotation occurred only in binary stars, perhaps because tidal forces produced synchronization of axial rotation and orbital revolution. Since the Sun has a very slow axial rotation (about *2km/sec* at its equator), most astrophysicists at the time believed that the rotation of all other single stars was probably also small. During 1930-1934, a systematic study of stellar rotation was undertaken by Struve in collaboration with Christian T. Elvey (1899-1972) and Miss Christine Westgate, at the Yerkes Observatory of the University of Chicago. The measurements were made by fitting the observed contour of a spectral line to a computed contour

obtained by applying different amounts of Doppler broadening to an intrinsically narrow line-contour having the same equivalent width as the observed line. They showed that the measured values of the rotational component of the velocity along the line of sight fell in the range 0-250 *km/sec* and may occasionally be as large as 400 *km/sec* or even more. A correlation of rotational velocities with spectral type was originally discovered by Struve and Elvey in 1931: the O-,B-,A- and early F-type stars frequently have large rotational velocities, while in late F-type stars and later types rapid rotation occurs only in close spectroscopic binaries. They also found that supergiants of early and late types, and normal giants of type F and later, never show conspicuous rotations.

At this juncture the problem was quietly abandoned for fifteen years. Interest in the measurements of axial rotation in stars was revived in 1949 by Arne Slettebak at Ohio State University.

1.3 Rotating Fluid Masses

Research into the influence of rotation upon the internal structure and evolution of a star has a long history. Sir Isaac Newton (1643-1727) was the first to realize the importance of the law of gravitation for the explanation of the figures of celestial bodies. He originally discussed the figure of the Earth in the *Philosophiae Naturalis Principia Mathematica* (Book III, Propositions 18-20, 1687) on the hypothesis that it might be treated as a homogeneous, slightly oblate spheroid rotating with constant angular velocity. Assuming that such a spheroid is a figure of equilibrium, Newton asserted that two perpendicular columns of fluid – one axial and the other equatorial – bored straight down to the Earth’s center must have equal weight. From this condition, he was able to derive the causal relationship $f = (5/4)m$ between the ellipticity f of a meridional section and the ratio m of the centrifugal force at the equator to (average) gravitational attraction on the surface.

Further progress was made by Christian Huygens (1629-1695) in his *Discours de la cause de la pesanteur*, which was published at Leiden in 1690. To him we owe a necessary condition for the relative equilibrium of a rotating mass of fluid – that the resultant force of the attraction and the centrifugal force at any point of the free surface must be normal to the surface at that point. Huygens never accepted that adjacent particles of matter attract each other, but he did admit the existence of an attracting force always directed to a fixed point. Accordingly, in one of his models, he assumed that the Earth’s gravity is a single, central force varying inversely as the square of the distance from its center. Thence, in making use of Newton’s principle of balancing columns, Huygens derived the relation $f = (1/2)m$ for his model, when departure from sphericity is small. As we now know, this is equivalent to the hypothesis that the density of the Earth is infinite at the center and it should be contrasted with Newton’s work in which it is assumed that the Earth is homogeneous in structure. In actual practice, the measured quantity f for the Earth is comprised between the values derived by Newton and Huygens for their two extreme models.

While Newton’s ideas led ultimately to contemporary mechanics, at this stage they did not gain immediate acceptance in Europe. During the first half of the eighteenth century, most continental scientists were strong advocates of a vortex theory that had been devised by René Descartes (1596-1650) in 1644. The Cartesians rejected Newton’s ideas mainly because attraction, regarded as a cause, was unintelligible and they somehow inferred from their systems of vortices that the Earth should be flatter at the equator. In 1730s, to settle the dispute between the Cartesians and Newtonians, geodetic expeditions were sent to different parts of the Earth to measure the length of an arc of meridian. The expedition to Lapland returned first and confirmed that the Earth is indeed flatter at the poles. Pierre Louis Moreau de Maupertuis (1698-1759) – its leader and the first Frenchman with the courage openly to declare himself a Newtonian – was called ”the great flattener.” At this time the vortex theory was a lost cause.

During 1737-1743, the most significant advances in the subject were made by Alexis-Claude Clairaut (1713-1765) in Paris and by Colin Maclaurin (1698-1746) in Edinburgh. Again to appreciate the importance of their discoveries, it must be borne in mind that the science of hydrostatics was then an imperfect theory. Actually, this early work was made without a clear understanding of the concept of internal pressure. Hence, whenever Clairaut and Maclaurin established a proposition, they had to rely upon Newton's principle of balancing columns, Huygens' principle of the plumb line, or both. As a matter of fact, necessary and sufficient conditions of hydrostatic equilibrium remained unknown until 1755, when Leonard Euler (1707-1783) definitively established the general equations of motion of an inviscid fluid.

As we have seen, Newton assumed without demonstration an oblate spheroid as a possible figure of equilibrium for a slowly rotating mass of fluid. In 1737, Clairaut obtained an expression for the attraction of a homogeneous spheroid at any point of its surface, when the body does not greatly depart from a sphere. To first order in the ellipticity, he then showed that Huygens' principle of the plumb line obtains at every point on the free surface of Newton's model.

This result was generalized in 1740 by Maclaurin, who completely solved the problem of the attraction of a homogeneous spheroid when departure from sphericity cannot be considered small. Again using Newton's principle of balancing columns, he proved that any oblate homogeneous spheroid is a possible figure of relative equilibrium. He also was successful in relating the angular velocity of rotation to the ellipticity of a meridional section. Finally, he demonstrated that at every point the direction of the plumb line is perpendicular to the free surface. The basic concept of level surfaces was also introduced by Maclaurin, who observed that at all depths the resultant body force is always normal to a surface belonging to a family of homothetic spheroids.

We now come to the brilliant treatise of Clairaut, *Théorie de la figure de la terre*) published in 1743. As far as our subject is concerned, the most interesting part of this book deals with the figures of equilibrium of slowly rotating, centrally condensed bodies – a problem hitherto practically untouched. Clairaut considered a self-gravitating configuration composed of quasi-spherical strata of varying densities. Given this assumption, he showed that the level surfaces necessarily coincide with the surfaces of equal density. On applying Huygens's principle of the plumb line to each level surface, he then proved that oblate spheroids are compatible with relative equilibrium and he derived an equation relating the varying ellipticity of the strata with their density. Finally, to first order in the ellipticity, he showed that the diminution of the surface effective gravity in passing from the poles to the equator varies as the square of the cosine of the latitude.

While all the ideas necessary for the general theory of rotating bodies were proposed by these pioneers, most of our knowledge on this subject derives from the contributions of the Marquis Pierre Simon de Laplace (1749-1827) and Adrien-Marie Legendre (1752-1833) over the period 1773-1793. To Legendre we owe the concept of gravitational potential and the general theory of the attraction of a homogeneous ellipsoid. This work eventually led him to introduce the polynomials that now bear his name. It was also Legendre's suggestion to identify the level surfaces of a uniformly rotating body with the condition that the sum of the gravitational and centrifugal potentials is constant over these surfaces. From this condition he was able to bring Clairaut's theory to its present form and to prove that the strata must be oblate spheroids when departure from sphericity is small. As for Laplace, his studies of the problem led him to introduce the spherical harmonics and the differential equation with which his name has since been associated. The well known proposition that the surfaces of equal pressure, the isopycnic and the level surfaces all coincide in a uniformly rotating figure of equilibrium was first demonstrated by Laplace. In 1825, as a by-product of his studies of Clairaut's, Laplace also introduced the concept of barotropes and he explicitly solved and discussed the spherical barotrope of index $n=1$.

All the foregoing results were included by Laplace in his impressive *Traité de mécanique*

céleste) (1799-1825), though he often forgot to give appropriate credit to the important contributions of his colleague Legendre. The differential equation that relates the gravitational potential at an internal point of a body to the density at that point was originally derived by Siméon-Denis Poisson (1781-1840) in 1829 and it has become a permanent part of the theory of self-gravitating bodies.

The next important discovery was made by Karl Jacobi (1804-1851), who pointed out, in 1834, that axially symmetric configurations are not the only admissible figures of equilibrium. Jacobi gave decisive evidence of a homogeneous ellipsoid with three unequal axes as a possible form of relative equilibrium for rotating bodies. The same year, Joseph Liouville (1809-1882) published the analytical proof of this statement and in 1843 he gave the first description of these ellipsoids in terms of their angular momentum. It was already known that, as the angular momentum increases from zero to infinity, the Maclaurin spheroids range from a sphere to an infinitely flat disc. As for the Jacobi ellipsoids, which range from an axially symmetric configuration to an infinitely long needle, Liouville found that they represent possible figures of equilibrium only for angular momenta greater than a threshold value.

No further progress was made until the problem was taken up, independently, by Alexandr Mikhailovich Liapunov (1857-1918) and Henri Poincaré (1854-1912). To Poincaré we owe the general theory of the equilibrium and stability of ellipsoidal forms and the concept of figures of bifurcation. In particular, he showed the existence of pear-shaped figures that branch off the sequence of Jacobi ellipsoids. As a matter of fact, the pear shaped figures had already been discovered during the previous year, 1884, by Liapunov. Unfortunately, the results of the Russian mathematician remained unknown to the Western scientists until his papers were translated into French, at the request of Poincaré himself. The Liapunov-Poincaré figures gave rise to extensive investigations, for it was then conjectured that they may eventually come apart in two detached masses rotating about each other. This theory of the origin of double stars was originally proposed by Lord Kelvin (William Thomson, 1824-1907) and Peter Guthrie Tait (1831-1901) in 1883. Sir James Hopwood Jeans (1877-1946) was its most ardent upholder during 1920s.

As for centrally condensed bodies that greatly depart from spherical symmetry, important discoveries were also made during the period 1885-1935, although they attracted much less attention. Indeed, the stratification of a rapidly rotating, inhomogeneous body is never known a priori and is to be found from the conditions of relative equilibrium. By using a method of successive approximations, Liapunov was the first to derive an exact theory of inhomogeneous bodies, in which the level surfaces differ but little from concentric ellipsoids. This work is undoubtedly a masterpiece of functional analysis, but is still difficult to use, in actual practise. For this reason, other methods were devised by Leon Lichtenstein (1878-1933) in Berlin and Leipzig and by Rolin Wavre (1896-1949) in Geneva. Most of these techniques have been now superseded by numerical computations. Nevertheless, they led to the discovery of a few fundamental theorems that form the basis of the theory of centrally condensed, rapidly rotating bodies. Particular mention should also be made of the French mathematician Pierre Dive, who made a thorough study of differential rotation. That kind of research was out of fashion in the mid-thirties and most of these classical results have been largely ignored over the past forty years.

1.4 The Golden Age of Stellar Rotation

Although the theory of rotating stars has greatly advanced during the past fifty years, the basic concepts underlying most of the contemporary researches were developed during the period 1919-1941. Let us briefly discuss these early studies.

At the turn of the century it was already clear that stars were gaseous and centrally condensed configurations. In 1919, Jeans conceived the idea that sequences of uniformly rotating, centrally

condensed bodies may not mirror the classical Maclaurin-Jacobi sequences. To illustrate the problem, he constructed various sequences of uniformly rotating polytropes, the polytropic index n being a measure of central condensation. He observed that for values of n larger than $n_c \simeq 0.8$ the Maclaurin-Jacobi pattern does not prevail. That is to say, when $n \geq n_c$ the sequences of uniformly rotating polytropes does not admit a point of bifurcation, but they instead terminate by the balancing of the gravitational and centrifugal accelerations at the equator. Jeans therefore concluded that if one imagines a slowly contracting sequence of such figures, equatorial break-up would eventually occur. In other words, any further contraction would result in matter being shed from the equator in a continuous stream, centrifugal force outweighing gravity at the equator. This semiquantitative picture led Struve to suggest in 1931 that Be stars are uniformly rotating B-type stars on the verge of equatorial break-up, surrounded by gaseous rings.

During the same period, as more was discovered about the physical processes that take place within a star, it also became clear that energy is transported by radiation – not by convection – in the main bulk of the vast majority of stars. In 1923, this result led Edward Arthur Milne (1896-1950) at Oxford, to build the first detailed model for a slowly rotating star in pure radiative equilibrium. Ten years later, the technique was generalized and applied to slightly distorted polytropes by the Indian astrophysicist Subrahmanyan Chandrasekhar. Most of the recent stellar models that do not greatly deviate from spherical symmetry rely upon these two pioneering studies.

The next important step in the elucidation of stellar rotation was made in Upsala by Hugo von Zeipel (1873-1959). In 1924, he proved the following theorem: If a chemically homogeneous star, rotating as a rigid body with angular velocity Ω , is in static radiative equilibrium, then the rate of liberation of energy ϵ_{Nuc} at any point in its interior must be given by

$$\epsilon_{Nuc} = constant \left(1 - \frac{\Omega^2}{2\pi G\rho} \right) \quad (3)$$

where G and ρ are, respectively, the constant of gravitation and the density at that particular point. It is evident that since the actual energy sources of a star do not fulfill condition (3), at least one of the foregoing assumptions must be relaxed. This fact was first discussed, independently, by Heinrich Vogt (1890-1968) in Heidelberg and by Sir Arthur Stanley Eddington (1882-1944) in Cambridge. In 1925, they showed that strict radiative equilibrium must necessarily break down in a uniformly rotating star. This, they argued, will upset the constancy of temperature and of pressure over the level surfaces; a pressure gradient will thus ensue, causing a flow of matter primarily in planes passing through the axis of rotation. A quantitative study of the physical properties of this meridional circulation was originally made by Eddington in 1929.

Finally no survey of this Golden age of stellar rotation would be complete without special mention of the Oslo school of fluid mechanics. To Vilhelm Bjerknes (1862-1951) we owe a systematic study of physical hydrodynamics. In particular, he laid the foundations of the theory of barotropes and baroclines and systematized the problem of the small oscillations of a continuous medium about a state of equilibrium. Although these questions were mainly discussed in the specific context of meteorology, they paved the road to many astrophysical applications. In this respect, let us mention the pioneering work of Svein Rosseland and Gunnar Randers. Of particular importance is the stability analysis of a rotating compressible fluid by Einar Hóiland (1907-1974) and Halvor Solberg (1895-1974). A first criterion was obtained by Solberg in 1936, for the case of axisymmetric disturbances in a rotating star with constant entropy. Under these conditions, he showed that the dynamical instability occurs if:

$$\frac{d}{d\varpi}(\Omega^2 \varpi^4) < 0 \quad (4)$$

where the angular velocity Ω is some specified function of the distance ϖ from the axis of rotation. In 1941 this result was generalized by Hóiland, who considered the case where Ω depends on the coordinate along the rotation axis, as well.

2 Permanent Rotations

2.1 Introduction

Let us consider a star for which rotational motion and magnetic field are completely negligible. Let us further assume that this star is isolated from other bodies. Then, as is well known, the system assumes a spherical shape, i.e. the surface upon which the total pressure p vanishes is a sphere. Moreover, the surfaces of constant pressure – isobaric surfaces – can be described by means of concentric spheres. In consequence, the gravitational potential V , the density ρ , the temperature T and the luminosity L also possess spherical symmetry. It is this geometric simplicity that renders the problem of the structure and evolution of radiating stars in hydrostatic equilibrium tractable.

Consider next a single star that rotates about a fixed direction in space with some assigned angular velocity. As we know, in the absence of a magnetic field, the star then becomes an oblate figure. We are at once faced with the following questions: what is the geometrical shape of the outer boundary? What is the form of the surfaces upon which the physical parameters of the star remain constant? To sum up what is the actual stratification of a rotating star and how does it depend on the angular velocity distribution? Obviously, the boundary is no longer spherical. Could we describe the isobaric surfaces by means of a set of suitable ellipsoids? Under very special circumstances, this is a possibility, but for an arbitrary rotating star, ellipsoids do not in general provide an acceptable approximation. At first glance, we could surmise the star to be symmetric with respect to its axis of rotation. This is not always the case, for models having a genuine triplanar symmetry may be constructed. Could we then at least expect the star to be symmetric with respect to a plane perpendicular to its axis of rotation? This is true provided that some stringent conditions are met. As a matter of fact, we have no a priori knowledge of the actual stratification in a rotating star. In general, the stratification is unknown and must be derived from the hydrodynamical equation of the problem. This situation is in sharp contrast to the case of a nonrotating star, for which a spherical stratification can be assumed *ab initio*.

At this stage, a further difficulty arises in the theory of stellar rotation. If we except stars that we assume to rotate as a rigid body, friction between the various layers induces a net transfer of angular momentum in the course of time. Hence, unless simplifying assumptions are made, we cannot expect to adequately approximate stars in a state of differential rotation by means of time-independent models. Specifically, if the time scale of friction is shorter than the lifetime of rotating star², angular momentum transfer has to be taken into account.

In view of the foregoing remarks, we cannot hope to investigate the structure and evolution of rotating stars to the same degree of generality obtained for stars in hydrostatic equilibrium. In the present chapter we explore some simple mechanical properties that are relevant to rotating stars. All of them can be derived without a detailed knowledge of stellar models.

2.2 Assumptions and Definitions

Let us first make the following assumption:

²Extensive researches of rotating neutron stars (NS) has shown that this is not actually true, i.e. the time scale of friction is larger than the lifetime of a rotating NS. Therefore, in this work we assume friction to be negligible.

- (i) *the star is isolated in space and rotates about a fixed axis with some yet unspecified angular velocity*
- (ii) *the system is stationary when viewed in an inertial frame of reference, and the density of each mass element remains a constant as we follow its motion*
- (iii) *friction may be neglected altogether*
- (iv) *no electromagnetic force is acting upon the star*

By definition, if a configuration satisfies all the aforementioned properties it is said to be in a state of permanent rotation for an inertial observer. Assume now the star to rotate about the z-axis and take the origin of our frame of reference at center of mass. Thus, in cylindrical coordinates (ϖ, ϕ, z) the components of the velocity \mathbf{v} have the form:

$$v_{\varpi} = 0, \quad v_{\phi} = \Omega\varpi, \quad v_z = 0, \quad (5)$$

in an inertial frame. For the present, the angular velocity Ω is an arbitrary function of spatial coordinates.

By virtue of the foregoing hypothesis, a first conclusion may be drawn at once:

If a gaseous star is in a state of permanent rotation when viewed in an inertial frame of reference, it necessarily possesses axial symmetry.

This result is a mere consequence of the conservation of mass. Indeed, we can write

$$\frac{D\rho}{Dt} + \rho \operatorname{div}\mathbf{v} = 0, \quad (6)$$

or

$$\frac{\partial\rho}{\partial t} + \mathbf{v} \cdot \operatorname{grad}\rho + \rho \operatorname{div}\mathbf{v} = 0 \quad (7)$$

Since, the density of a mass element does not vary along its path, we have $\frac{D\rho}{Dt} = 0$. Despite the gaseous nature of the system equation 6 thus implies

$$\operatorname{div}\mathbf{v} = 0 \quad (8)$$

From equations 5 and 8 we obtain

$$\Omega = \text{constant} \quad \eta' \quad \Omega = \Omega(\varpi, z) \quad (9)$$

Now, in view of assumption (ii), we also have $\partial\rho/\partial t = 0$ and therefore equations 7 and 8 give

$$\mathbf{v} \cdot \operatorname{grad}\rho = 0. \quad (10)$$

This equation shows that the velocity \mathbf{v} lies in a plane tangent to the surfaces of equal density. Thus, by virtue of equations 5, 9 and 10 we can write

$$\Omega \frac{\partial\rho}{\partial\phi} = 0 \quad (11)$$

and assuming that Ω does not vanish, we find

$$\rho = \rho(\varpi, z) \quad (12)$$

In making use of equations 9 and 12 we can easily show that the functions p, V, T and L possess axial symmetry³.

The foregoing conclusion greatly simplifies the equations of motion (Euler's equations):

$$\frac{1}{\rho} \frac{\partial p}{\partial \varpi} = -\frac{\partial V}{\partial \varpi} + \Omega^2 \varpi, \quad (13)$$

and

$$\frac{1}{\rho} \frac{\partial p}{\partial z} = -\frac{\partial V}{\partial z} \quad (14)$$

In general, the gravitational potential and density are related by the Poisson equation

$$\nabla^2 V = 4\pi G \rho, \quad (15)$$

where G represents the constant of gravitation. Instead of equation 15, it is some times more convenient to use the integral form of the Newtonian potential i.e.,

$$V(\varpi, z) = -G \int_{\mathcal{V}} \frac{\rho(\mathbf{x}')}{|\mathbf{x} - \mathbf{x}'|} d\mathbf{x}', \quad (16)$$

where the triple integral must be evaluated over the unknown volume \mathcal{V} of the star. By convention, the stellar boundary corresponds to the surface \mathcal{Q} upon which the pressure vanishes. The integral form 16 has the advantage that it incorporates ipso facto the boundary conditions on the gravitational potential, i.e. the continuity of gravity across the (unknown) surface \mathcal{Q} .

To complete the formulation of the problem, we must now include an appropriate equation of state. In general the pressure depends on the density, temperature and chemical composition of the star. At this stage, an explicit relation is not needed and we write symbolically

$$p = p(\rho, T, \lambda_1, \lambda_2, \dots), \quad (17)$$

where λ 's denote a set of variables which generally depend on ϖ and z . By definition, we call barocline (or baroclinic star) a system for which a physical relation of the form 17 holds. Naturally, the temperature is an additional unknown quantity. Hence, even if we know the λ 's, another thermodynamical equation must be written down to complete our set of equations. For the time being, we shall not need such a relation.

Under special circumstances, it is convenient to complement the equations of motion by means of a geometrical relation between just the pressure and density. We assume that

$$p = p(\rho). \quad (18)$$

Every model for which such a relation exists is called a barotrope (or barotropic star). As an example, we can mention the polytropes that, in many instances, serve a useful purpose in that they represent simple systems. Naturally, a zero temperature white dwarf also satisfies an equation of barotropy. However, physically, it should rather be viewed as a particular limit of a barocline.

The basic distinction between barotropes and baroclines naturally lies in their respective stratification. Obviously, the surfaces of equal density – the isopycnic surfaces – and the isobaric surfaces coincide in a barotropic star. On the contrary, isopycnic surfaces are in general inclined to and cut the isobaric surfaces in a baroclinic star. In the latter case, coincidence sometimes occurs under very specific conditions.

³It is impossible to build steady models for which axial symmetry does not exist. However, these configurations are time independent when viewed from a suitably chosen rotating frame of reference.

2.3 Barotropes, Pseudo-Barotropes and Baroclines

Many useful properties can be deduced from equations 13 and 14. For this purpose, let us first define the effective gravity \mathbf{g} as the gravitational attraction per unit mass corrected for the centrifugal acceleration. In cylindrical coordinates, we thus have

$$g_{\varpi} = -\frac{\partial V}{\partial \varpi} + \omega^2 \varpi \quad (19)$$

$$g_z = -\frac{\partial V}{\partial z} \quad (20)$$

Accordingly, equations 13 and 14 can be rewritten as:

$$\frac{1}{\rho} \text{grad } p = \mathbf{g} \quad (21)$$

A first conclusion can readily be made:

Given a star in a state of permanent rotation, the effective gravity is everywhere orthonormal to the isobaric surfaces

This property is valid for both barotropic and baroclinic stars.

The Poincaré-Wavre Theorem

Let us now assume the star to rotate as a rigid body. Equations 19 and 20 then become

$$\mathbf{g} = -\text{grad}\Phi, \quad (22)$$

where, except for an additive constant, we have

$$\Phi(\varpi, z) = V(\varpi, z) - \frac{1}{2}\Omega^2\varpi^2. \quad (23)$$

Consider next a differentially rotating star. Under what circumstances can one also derive the effective gravity from a potential? By virtue of equation 20, this is possible if and only if Ω does not depend on z , i.e., when the angular velocity is a constant over cylindrical surfaces centered about the axis of rotation. Instead of equation 23 we obtain

$$\Phi(\varpi, z) = V(\varpi, z) - \int^{\varpi} \Omega^2(\varpi')\varpi' d\varpi'. \quad (24)$$

As we shall presently see, various interesting conclusions can be inferred from the existence of such a potential.

First of all, by virtue of 21 we can always write

$$\frac{1}{\rho} dp = g_{\varpi} d\varpi + g_z dz. \quad (25)$$

Using equations 22 and 24 we thus find that

$$\frac{1}{\rho} dp = -d\Phi \quad (26)$$

By definition, for any displacement on a level surface $\Phi = \text{constant}$, we have $d\Phi = 0$. Since the foregoing equation shows that $dp = 0$ on the same surface, the isobaric surfaces coincide with the level surfaces. Hence, we have

$$p = p(\Phi) \quad \eta' \quad \Phi = \Phi(p) \quad (27)$$

and

$$\frac{1}{\rho} = -\frac{d\Phi}{dp}. \quad (28)$$

Therefore, the density is also a constant over a level surface. In conclusion, the surfaces upon which p, ρ and Φ remain constant all coincide. As a consequence, when a potential Φ does exist, the vector \mathbf{g} is normal to the isopycnic surfaces.

Reciprocally, let us consider a star for which the isobaric and isopycnic surfaces coincide. If we let

$$\Phi(p) = -\int \frac{dp}{\rho(p)}, \quad (29)$$

equation 25 becomes:

$$d\Phi = -g_{\varpi}d\varpi - g_z dz. \quad (30)$$

The quantity $d\Phi$ is an exact total differential. Accordingly equation 22 must hold true and \mathbf{g} may be derived from a potential.

Finally, let us suppose that the effective gravity is everywhere normal to the isopycnic surfaces. By virtue of equation 25, we see that the pressure is a constant over such a surface. The coincidence of isobaric and isopycnic surfaces is thus established.

If we now collect all the pieces, it is a simple matter to see that we have proved the following theorem that bears the title "The Poincaré-Wavre Theorem"

Theorem 1 *For a star in a state of permanent rotation, any of the following statements implies the three others: (i) the angular velocity is a constant over cylinders centered about the axis of rotation, (ii) the effective gravitational acceleration can be derived from a potential, (iii) the effective gravity is normal to isopycnic surfaces, (iv) the isobaric and isopycnic surfaces coincide.*

These important results were first proved by Poincaré and Wavre.

One would be tempted to conclude that these four equivalent propositions refer solely to barotropes, and exclude altogether baroclinic stars. This is not quite true. To prove it, consider again a system for which Ω depends on both ϖ and z . If we eliminate the gravitational potential V from equations 13 and 14 we may write

$$\frac{\partial}{\partial z}(\Omega^2\varpi) = \frac{\partial}{\partial z} \left(\frac{1}{\rho} \right) \frac{\partial p}{\partial \varpi} - \frac{\partial}{\partial \varpi} \left(\frac{1}{\rho} \right) \frac{\partial p}{\partial z} \quad (31)$$

Returning to equation 5 we obtain

$$2\frac{\partial\Omega}{\partial z}\mathbf{v} = \text{grad}\frac{1}{\rho} \times \text{grad}p. \quad (32)$$

This equation readily shows that isobaric and isopycnic surfaces all coincide if and only if

$$\frac{\partial\Omega}{\partial z} = 0 \quad (33)$$

This is a direct consequence of the equations of motion and requires no prior knowledge of the equation of state (EOS).

Clearly, condition 33 is always true for barotropes in uniform or nonuniform rotation. However, if we consider a rotating barocline for which we impose condition 33, equation 31 shows that the isobaric and isopycnic surfaces must also coincide in that case – although this is most

unnatural and not required a priori by the EOS that relates p, ρ, T and possibly other parameters! Thus, in general, we can assert that

Whatever the EOS, baroclinic stars for which $\partial\Omega/\partial z = 0$, are characterized by the following properties: (i) the effective gravity can be derived from a potential, (ii) the effective gravitational acceleration is normal to the isopycnic surfaces and (iii) the isobaric and isopycnic surfaces always coincide.

Henceforth, these very peculiar baroclines will be called "pseudo-barotropes" for they share most of the properties of barotropes. They should be contrasted with true baroclines about which we can now make the following statement:

Given a nonuniformly rotating baroclinic star for which the angular velocity depends on both ϖ and z , (i) the effective gravity cannot be derived from a potential, (ii) in no case is the effective gravity normal to the isopycnic surfaces and (iii) the isobaric and isopycnic surfaces are always inclined to each other by a finite angle.

In summary, if we exclude the peculiar case of pseudo-barotropes, we can say that barotropic stars are characterized by the two equivalent statements

$$\frac{\partial\Omega}{\partial z} = 0 \quad \kappa\alpha \quad p = p(\rho) \tag{34}$$

Furthermore, for both barotropes and pseudo-barotropes, the stratification is such that the surfaces upon which p, ρ and Φ assume a constant value coincide. Also the lines of force of the effective gravity are orthogonal to these surfaces. The above properties will greatly simplify the problem of constructing rotating configurations. On the contrary, matters are not that simple when we consider genuine baroclines for, then, none of the above properties remains true. Of particular importance is the fact that the effective gravity ceases to be orthogonal to the isopycnic surfaces.

The Lichtenstein Theorem

A further distinction between barotropes and baroclines is the existence or not of an equatorial plane of symmetry. Contrary to a current belief, this is far from being a trivial question, for such a plane may not exist. The problem was thoroughly investigated by Lichtenstein and Wavre, who have proved that

Rotating stars, for which the angular velocity does not depend on z , always possess an equatorial plane of symmetry, which is perpendicular to the axis of rotation.

A rigorous mathematical demonstration of this theorem is outside the scope of this work. As expected, the case of genuine baroclines is somewhat more involved. Indeed, the angular velocity then depends on both ϖ and z . Again omitting the proof, we can summarize the result in the following statement:

Theorem 2 *Given a differentially rotating barocline, if the angular velocity is everywhere a single valued function of density and the distance ϖ from the axis, then the body is symmetric with respect to an equatorial plane.*

In other words, consider an arbitrary line that is parallel to the rotation axis. Whenever it crosses the body it intersects each isopycnic surface at two points. If $\Omega(\varpi, z)$ assumes the same value at these two points, $\Omega(\rho, \varpi)$ is a single-valued function and this ensures the existence of a plane of symmetry. The question was originally discussed by Dive.

2.4 Spheroidal Stratifications

At this point, it is of some relevance to ask under what conditions isobaric surfaces can be described by means of a suitable set of concentric spheroids. The question was first raised by Hamy in 1889 and is not as simple as it may first appear. To illustrate the problem, let us again restrict ourselves to uniformly rotating stars. By virtue of equation 15 on applying the Laplacian operator to both sides of equation 23, we obtain

$$\nabla^2\Phi = 4\pi G\rho - 2\Omega^2 \quad (35)$$

Moreover, for uniformly rotating bodies, the density is only a function of Φ . Hence, equation 35 can be written symbolically in the form

$$\frac{\partial^2\Phi}{\partial\varpi^2} + \frac{1}{\varpi} \frac{\partial\Phi}{\partial\varpi} + \frac{\partial^2\Phi}{\partial z^2} = f(\Phi) \quad (36)$$

Quite generally, we now assume as did Voltera and Pizzetti, that the level surfaces $\Phi = \text{constant}$ are given by

$$F(\varpi, z, \Phi) = 0 \quad (37)$$

where, for the time being the above function remains unspecified. We can thus write

$$\frac{\partial F}{\partial\varpi} + F' \frac{\partial\Phi}{\partial\varpi} = 0, \quad (38)$$

where a dash denotes a derivative with respect to Φ . We also have

$$\frac{\partial^2 F}{\partial\varpi^2} + 2 \frac{\partial F'}{\partial\varpi} \frac{\partial\Phi}{\partial\varpi} + F' \frac{\partial^2\Phi}{\partial\varpi^2} + F'' \left(\frac{\partial\Phi}{\partial\varpi} \right)^2 = 0 \quad (39)$$

and two similar equations in which ϖ is replaced by z . Using these four equations to eliminate the derivatives of Φ in equation 36, we eventually obtain

$$F'^2 \nabla^2 F - 2F' \left(\frac{\partial F}{\partial\varpi} \frac{\partial F'}{\partial\varpi} + \frac{\partial F}{\partial z} \frac{\partial F'}{\partial z} \right) + F'' \left[\left(\frac{\partial F}{\partial\varpi} \right)^2 + \left(\frac{\partial F}{\partial z} \right)^2 \right] + F'^3 f = 0 \quad (40)$$

Clearly, if the assigned stratification provides an acceptable solution, equation 40 must be identically satisfied for all ϖ, z and Φ related by equation 37.

Choose now a spheroidal stratification of the form

$$F(\varpi, z, \Phi) = \alpha(\Phi)\varpi^2 + z^2 - h(\Phi) = 0 \quad (41)$$

where α and h designate two arbitrary functions of Φ . Equation 40 thus becomes

$$2(2\alpha + 1)(a'\varpi^2 - h')^2 - 8(a'\varpi^2 - h')\alpha\alpha'\varpi^2 + 4(\alpha''\varpi^2 - h'')[\alpha(\alpha - 1)\varpi^2 + h] + (a'\varpi^2 - h')^3 f = 0 \quad (42)$$

from which we have already eliminated the variable z . The foregoing equation must be satisfied for all values of ϖ , if spheroids are to provide an acceptable solution.

The last term in equation 42 is of degree six in ϖ , while the remaining terms are of degree four in the same variable. We conclude that

$$\alpha' = 0 \quad \eta' \quad \alpha = \sigma\tau\alpha\theta\epsilon\rho\alpha' \quad (43)$$

Spheroids 41 must be homothetic and equation 42 reduces to

$$2(2\alpha + 1)h'^2 - 4h''[\alpha(\alpha - 1)\varpi^2 + h] - h'^3 f = 0 \quad (44)$$

We naturally exclude $\alpha = 1$ as a possible solution, for it corresponds to a spherical stratification. Hence, we are left with the choice

$$h'' = 0 \quad \eta' \quad h' = \sigma\tau\alpha\theta\epsilon\rho\alpha' \quad (45)$$

and therefore, we must also assume that f is a constant. In view of equations 35 and 36, this implies in turn that ρ must be a constant. In conclusion, the sole acceptable solutions are uniformly rotating spheroids of constant density, with the pressure being a constant over homothetic spheroids.

Similarly, one can show that differentially rotating stars for which Ω depends only on ϖ , do not allow for spheroidal stratifications. The proof will be omitted here. Nevertheless, we can now enunciate a general proposition:

Given a centrally condensed barotrope or pseudo-barotrope in a state of permanent rotation, the isobaric surfaces cannot be described by means of a set of concentric spheroids.

This result calls for two remarks. First, if we assume that departure from sphericity is small, spheroidal stratifications can be used to describe slowly rotating bodies in a first approximation. Second, the foregoing proposition does not apply to genuine baroclines. This was originally shown by Dive. Actually, many such models can be constructed by using appropriate spheroidal stratification. However, realistic stellar models cannot be adequately described by means of these simple solutions.

2.5 Some Inequalities

From a purely mechanical point of view, the specification of a particular model in a state of permanent rotation depends on three quantities: (i) the total mass M , (ii) the total angular momentum J and (iii) an assigned distribution for the angular momentum per unit mass.⁴ Consider now a fixed value of M and a given rotation field and construct a sequence of models along which J increases. Besides J , what is the most convenient parameter that characterizes the gross features of a model along the sequence? In the case of a spheroid, we could naturally use the eccentricity of a meridional section, but this is not very suitable when we are dealing with an object for which the boundary is numerically defined. We could also use the equatorial angular velocity Ω_e . Again, this is not the best choice, since Ω_e does not monotonically increase with J . Another possibility is provided by the ratio of the rotational kinetic energy K to the gravitational potential energy W , i.e

$$\tau = \frac{K}{W} \quad (46)$$

where

$$K = \frac{1}{2} \int_{\mathcal{V}} \rho \Omega^2 \varpi^2 \mathbf{d}\mathbf{x}, \quad (47)$$

⁴The fact that we neglect friction compels us to describe the dependence of the angular momentum per unit mass on the coordinates. Only when viscous effects are taken into account can the rotation field be deduced from the hydrodynamical equations and the boundary conditions.

and

$$W = \frac{1}{2} \int_{\mathcal{V}} \rho V \mathbf{d}\mathbf{x} \quad (48)$$

By virtue of the scalar Virial theorem, we have

$$2K - |W| + 3 \int_{\mathcal{V}} p \mathbf{d}\mathbf{x} = 0 \quad (49)$$

As the volume integral over the pressure always remains a non-negative quantity, we can thus write

$$|W| - 2K \geq 0 \Rightarrow 0 \leq \tau \leq \frac{1}{2} \quad (50)$$

Of course, at this stage we do not know a priori whether the entire domain of values for τ (or J) can be covered by suitable models.

To justify our choosing τ as a convenient parameter, let us illustrate the problem by means of uniformly rotating, homogeneous spheroids, i.e. Maclaurin spheroids. Their existence was proved in the previous section. Their actual derivation is straightforward for the gravitational attraction in a homogeneous spheroid. We have

$$\frac{\partial V}{\partial \varpi} = 2\pi G \rho A_1 \varpi \quad \kappa \alpha_1 \quad \frac{\partial V}{\partial z} = 2\pi G \rho A_3 z \quad (51)$$

where

$$A_1(e) = \frac{(1 - e^2)^{1/2}}{e^3} \sin^{-1} e - \frac{1 - e^2}{e^2} \quad (52)$$

and

$$A_3 = \frac{2}{e^2} - \frac{2(1 - e^2)^{1/2}}{e^3} \sin^{-1} e. \quad (53)$$

The eccentricity e is given by

$$e = (1 - \alpha_3^2/\alpha_1^2)^{1/2}, \quad (54)$$

where α_1 and α_3 denote the two semi axes of a meridional section ($\alpha_3 \leq \alpha_1$). Both the gravitational attraction and the centrifugal force are linear in the coordinates. Hence, in view of equations 13 and 14, the pressure must be a quadratic form

$$p(\varpi, z) = 2\pi G \rho^2 \alpha_3^2 A_3 \left(1 - \frac{\varpi^2}{\alpha_1^2} - \frac{z^2}{\alpha_3^2} \right) \quad (55)$$

This result is in agreement with equation 43. We also have

$$\frac{\Omega^2}{2\pi G \rho} = A_1 - (1 - e^2) A_3, \quad (56)$$

$$\tau = \frac{A_1 - (1 - e^2) A_3}{2A_1 + (1 - e^2) A_3}, \quad (57)$$

and

$$\frac{J}{(GM^3\bar{\alpha})^{1/2}} = \frac{\sqrt{6}}{5}(1 - e^2)^{-1/3}[A_1 - (1 - e^2)A_3]^{1/2}, \quad (58)$$

where $\bar{\alpha} = (\alpha_1^2\alpha_3)^{1/3}$. Figures 1 and 2 illustrate the behavior of e , $f [= (1 - \alpha_3/\alpha_1)]$, J and Ω^2 as a function of τ . The eccentricity e and the ellipticity f vary from zero to 1, while J increases from zero to infinity. Models can thus be constructed for all values of J . They range from a sphere to an infinitesimally flat disc. When expressed as a function of τ , Ω^2 at first increases, then reaches a maximum and from there monotonically decreases along the sequence.

Maclaurin spheroids closely imitate in all essential respects sequences of differentially rotating centrally condensed barotropes. On the contrary, for stellar models in uniform rotation, the sequences usually terminate well before the limit $\tau = 1/2$ may be reached. In all cases, the angular velocity never increases from zero to infinity. In view of these anticipated results, it would be desirable to derive at this stage an upper limit to the angular velocity without prior knowledge of the detailed structure of a model.

Consider a uniformly rotating star with an otherwise unspecified mass distribution. If we integrate equation 35 over the entire volume \mathcal{V} we find

$$\oint_{\mathcal{Q}} \frac{d\Phi}{dn} dS = 4\pi GM - 2\Omega^2\mathcal{V}. \quad (59)$$

In establishing equation 59 we made use of the following relations:

$$\int_{\mathcal{V}} \nabla^2 \Phi d\mathbf{x} = \int_{\mathcal{V}} \text{div grad } \Phi d\mathbf{x} = \oint_{\mathcal{Q}} \text{grad } \Phi \cdot d\mathbf{S} = \oint_{\mathcal{Q}} \frac{d\Phi}{dn} dS, \quad (60)$$

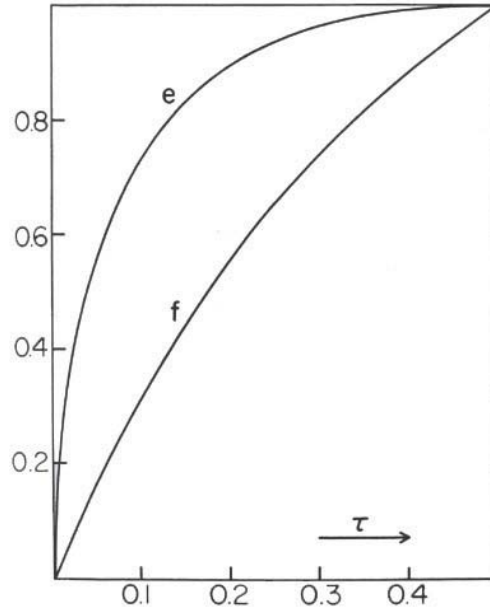


Figure 1: The eccentricity e and the ellipticity f along the Maclaurin sequence, as a function of $\tau = K/|W|$.

where n is the outer normal to the surface. Clearly, a necessary condition for equilibrium is that the effective gravity \mathbf{g} be directed inwards at every point on the surface. Thus, we must have

$$\oint_{\mathcal{Q}} \frac{d\Phi}{dn} dS > 0, \quad (61)$$

or, in view of equation 59,

$$\Omega^2 < 2\pi G\bar{\rho}, \quad (62)$$

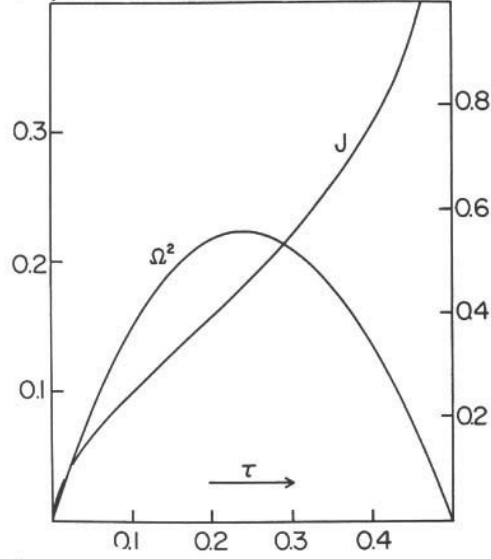


Figure 2: The squared angular velocity Ω^2 and the total angular momentum J along the Maclaurin sequence, as a functions of $\tau = K/|W|$. Ordinates on the left and on the right refer to Ω^2 and J , respectively

where $\bar{\rho}$ denotes the mean density M/V . Inequality 62 was originally derived by Poincaré in 1885.

A grweat deal of effort has been spent refining the foregoing inequality. Under similar assumptions Crudeli and Nikliborc proved that

$$\Omega^2 < \pi G\rho_c, \quad (63)$$

where ρ_c is the central density – if we assume that ρ monotonically decreases as we move outwards. Clearly, equation 63 is no better than equation 62 when $\rho_c/\bar{\rho} > 2$. In 1959 Quilghini obtained the new limit

$$\Omega^2 < \pi G\bar{\rho}, \quad (64)$$

which is a definite improvement but still well above the maximum value attained by Ω^2 for Maclaurin spheroids i.e. $\Omega^2 \approx 0.45\pi G\bar{\rho}$.

Turning next to barotropes and pseudo-barotropes in a state of differential rotation, we must naturally use equation 24. Then, instead of equation 35 we have

$$\nabla^2\Phi = 4\pi G\rho - 2\Omega^2 - \varpi \frac{d\Omega^2}{d\varpi}, \quad (65)$$

and inequality 62 becomes

$$\nu^{-1} \int_{\nu} \left(\Omega^2 + \frac{1}{2} \varpi \frac{d\Omega^2}{d\varpi} \right) \mathbf{d}\mathbf{x} < 2\pi G\bar{\rho}. \quad (66)$$

The foregoing criterion is due to Wilczynski. Moreover, for any differentially rotating star, it can be proved that

$$\Omega_{min}^2 + \frac{1}{2}g_{min} \frac{\mathcal{O}}{\mathcal{V}} < 2\pi G\bar{\rho} < \Omega_{max}^2 + \frac{1}{2}g_{max} \frac{\mathcal{O}}{\mathcal{V}}. \quad (67)$$

The quantities Ω_{min} and Ω_{max} designate, respectively, the minimum and maximum values of Ω on the surface. Similarly, g_{min} and g_{max} are the extreme values of $|\mathbf{g}|$, while \mathcal{O} denotes the area of the surface. These limitations have been derived by Dive.

2.6 The Outer Gravitational Field

As we know, the gravitational field exterior to a spherical distribution of matter depends solely on the total mass M of the attracting body. Now, on what elements does the outer gravitational field of a rotating star depend? The question was first raised by Stokes in 1849 and a clear-cut answer was originally given by Poincaré. The following statement can be made and is due to Wavre:

The outer gravitational field due to a rotating star is entirely determined by the total mass M , the shape of the boundary \mathcal{Q} and the distribution of angular velocity on the surface of the star.

Leaving aside some mathematical subtleties, the proof is straightforward. By virtue of equations 13 and 14 we can always write

$$\frac{1}{\rho}dp = -dV + \Omega^2\varpi d\varpi, \quad (68)$$

where $\Omega^2(\varpi, z)\varpi$ is not in general derived from a potential. Let draw a line ℓ on the surface of the star. Along that arbitrary line, we always have $dp = 0$. Hence, we obtain

$$dV_s = \Omega_s^2\varpi d\varpi, \quad (69)$$

where the subscript s indicates a value on the surface \mathcal{Q} . Integrate next along the line ℓ from a fixed point P_o to a variable point P , and let

$$\Gamma = \int_{P_o}^P \Omega_s^2\varpi d\varpi. \quad (70)$$

Because V_s is a single-valued function and dV_s an exact total differential, the line integral Γ only depends on the limiting points P_o and P , and is independent of the path of integration drawn on the surface. We thus have

$$V_s(P) = V_s(P_o) + \Gamma(P_o, P). \quad (71)$$

Now, the outer gravitational potential V_E can always be written in the form ⁵

$$V_E(\mathcal{A}) = -\frac{1}{4\pi} \oint_{\mathcal{Q}} \frac{1}{D} \left(\frac{dV}{dn} \right)_s dS + \frac{1}{4\pi} \oint_{\mathcal{Q}} V_s \frac{d}{dn} \left(\frac{1}{D} \right) dS, \quad (72)$$

where D denotes the distance from an external point \mathcal{A} to the point P . Also, in virtue of equation 15, we obtain

$$M = \frac{1}{4\pi G} \oint_{\mathcal{Q}} \left(\frac{dV}{dn} \right)_s dS. \quad (73)$$

⁵See e.g. [2] pp. 218-223.

Substituting equation 71 into equation 72, we find

$$V_E(\mathcal{A}) = -\frac{1}{4\pi} \oint_{\mathcal{Q}} \frac{1}{D} \left(\frac{dV}{dn} \right)_s dS + \frac{1}{4\pi} \oint_{\mathcal{Q}} \Gamma(P, P_o) \frac{d}{dn} \left(\frac{1}{D} \right) dS, \quad (74)$$

for $V(P_o)$ is a constant and $1/D$ is an harmonic function. In view of equation 73, $(dV/Dn)_s$ is entirely determined by a knowledge of M and \mathcal{Q} . Thus, the first integral on the RHS of equation 74 is a function of M and \mathcal{Q} only. The second term in this equation depends solely on \mathcal{Q} and $\Omega_s(\varpi, z)$. This concludes the proof.

In summary, as in the case of a spherical body, no firm conclusion regarding the internal stratification can be inferred from the sole knowledge of its outer gravitational field. This precludes any investigation of the interior of the Sun – or, for that matter, of a planet – by means of a space probe.

2.7 Integral of Motion

In this subsection we will prove a very useful integral of motion, in the special case of axial rotation of a fluid mass.

The general equations of motion of a fluid are the Euler equations.

$$\frac{d\vec{u}}{dt} = \vec{f} - \frac{1}{\rho} \vec{\nabla} p \quad (75)$$

If the flow is stationary, then

$$\frac{\partial \vec{u}}{\partial t} = 0 \quad (76)$$

If the force can be derived from a potential

$$\vec{f} = -\vec{\nabla} \Phi \quad (77)$$

For a barotropic EOS we can always write

$$P = P(\rho) \Rightarrow \frac{\vec{\nabla} P}{\rho} = \vec{\nabla} \Pi, \quad \Pi = \int \frac{dP}{\rho} \quad (78)$$

Finally, if the configuration assumes axial symmetry, we can write in cylindrical coordinates (ϖ, ϕ, z) :

$\vec{u} = u_\phi(\varpi) \hat{e}_\phi$, $\vec{\omega} = \Omega(\varpi) \hat{e}_z$ ⁶ and

$$u_\phi(\varpi) = \Omega(\varpi) \varpi \quad (79)$$

By virtue of the foregoing equations, the LHS of equations 75 becomes

$$\vec{a} = \frac{d\vec{u}}{dt} = \frac{\partial \vec{u}}{\partial t} + (\vec{u} \cdot \vec{\nabla}) \vec{u} = 0 + u_\phi \frac{1}{\varpi} \frac{\partial}{\partial \phi} u_\phi(\varpi) \hat{e}_\phi = \frac{u_\phi^2}{\varpi} \frac{\partial \hat{e}_\phi}{\partial \phi} \quad (80)$$

However, in cylindrical coordinates, the following relations hold true

$$x = \varpi \sin \phi, \quad y = \varpi \cos \phi, \quad z = z \quad (81)$$

⁶Where the hat over an arbitrary vector denotes a unit vector

$$\hat{e}_\varpi = \vec{e}_\varpi = \frac{\partial \vec{r}}{\partial \varpi} = \sin \phi \hat{x} + \cos \phi \hat{y} \quad (82)$$

$$\vec{e}_\phi = \frac{\partial \vec{r}}{\partial \phi} = \varpi(\cos \phi \hat{x} - \sin \phi \hat{y}) \Rightarrow \hat{e}_\phi = (\cos \phi \hat{x} - \sin \phi \hat{y})$$

$$\hat{e}_z = \vec{e}_z = \frac{\partial \vec{r}}{\partial z} = \hat{z} \quad (83)$$

Now, if we differentiate \hat{e}_ϕ with respect to ϕ and make use of equation 82, we obtain

$$\frac{\partial \hat{e}_\phi}{\partial \phi} = -\hat{e}_\varpi \quad (84)$$

Thus, equation 80 becomes

$$\vec{a} = \frac{d\vec{u}}{dt} = -\frac{u_\phi^2}{\varpi} \hat{e}_\varpi = -\Omega^2 \varpi \hat{e}_\varpi \quad (85)$$

By combining equation 77, 78 and 85, equation 75 can be written as follows

$$\vec{\nabla} \Phi + \vec{\nabla} \Pi - \Omega^2 \varpi \hat{e}_\varpi = 0 \Rightarrow \quad (86)$$

$$\vec{\nabla} \Phi + \vec{\nabla} \Pi - \vec{\nabla} \int \Omega^2 \varpi d\varpi = 0 \quad (87)$$

We eventually obtain the integral of motion for axisymmetrically rotating fluid masses

$$\Phi + \Pi - \int \Omega^2 \varpi d\varpi = \text{const.} \quad (88)$$

3 Stellar Models - Techniques

Perturbation techniques are particular well suited to determine the equilibrium structure of barotropes and pseudo-barotropes, for which the level surfaces slightly depart from spheres. Of course, higher order corrections can be included to allow for larger distortions, but then, the analytical calculations become hopelessly prohibitive. For that reason, in order to make further progress, the problem should be viewed from another angle.

In this chapter we will present two techniques for simulating models of rotating stars. The first is the Self-Consistent Field method, which is abbreviated by *SCF* and the second one is a variant of the aforementioned method, devised by Izumi Hachisu. Henceforth, we will refer to the latter method as *HSCF*. Although these two techniques bear little difference, we quote the SCF method, so that the HSCF method, which is the one used in this project, becomes clearer.

3.1 The Self-Consistent Field Method (SCF)

The SCF method (which has been originally applied to barotropic and pseudo-barotropic stars by Ostriker and his associates) provides such a new approach, for it is especially designed to relax the restrictive assumption of quasi-sphericity. Moreover, since it requires a knowledge of the angular momentum distribution, it can treat differentially rotating models without any additional labor.

To illustrate the main features of this technique, let us restrict ourselves to the simple case of differentially rotating barotropes. The total mass M and the total angular momentum are considered to be fixed quantities. We designate by R the maximum radius of the barotrope under consideration. (Note that for severely distorted models which present anequatorial cusp, R may be greater than the equatorial radius.) Both cylindrical and spherical coordinates will be used with the standard notations. For further use, let m_{ϖ} be the fractional mass interior to the cylinder of radius ϖ . We have

$$m_{\varpi} = \frac{2\pi}{M} \int_0^{\varpi} \int_{-\infty}^{+\infty} \varpi' \rho(\varpi', z') d\varpi' dz'. \quad (89)$$

Consider now a barotrope on which we impose a rotation with some assigned velocity distribution. Hence, the angular momentum distribution per unit mass is

$$j = j(\varpi) = \Omega(\varpi) \varpi^2. \quad (90)$$

(By virtue of our approximations, remember that the angular velocity cannot depend on z , and must be specified a priori: cf. §§ 2.3 and 2.5.) We prescribe j as a function of the Lagrangian variable m_{ϖ} rather than as a function of ϖ . Thus, we can define the rotational motion by means of a function of the form

$$j = j(m_{\varpi}). \quad (91)$$

The above specification is particularly convenient when departure from sphericity is large. For the time being, we do not need to choose an explicit form for the function $j(m_{\varpi})$.

If we now let

$$U_{rot}(\varpi) = \int_0^{\varpi} \frac{j^2(m_{\varpi'})}{\varpi'^3} d\varpi', \quad (92)$$

and

$$V(\varpi, z) = -G \int_{\mathcal{V}} \frac{\rho(\mathbf{x}')}{|\mathbf{x} - \mathbf{x}'|} d\mathbf{x}', \quad (93)$$

the total potential becomes (cf. equation 24)

$$\Phi(\varpi, z) = V(\varpi, z) - U_{rot}(\varpi) \quad (94)$$

As we know, for a barotropic star the isopycnic and isobaric surfaces coincide with the level surfaces $\Phi = constant$. Therefore, ρ can be viewed as a function of Φ only i.e.

$$\rho = \rho(\Phi) \quad (95)$$

with the requirement that $\rho(\Phi_s) = 0$, where s designates, as usual, a value measured on the free surface of the star. Also, by virtue of equations 92 and 93, the functions Φ, ρ and j are related through potential theory by an integral operator. Consequently, V and U_{rot} at a given point depend for the most part on mean properties of the material interior to that point, rather than on local properties. Symbolically, we have

$$\Phi = \Phi(\rho; j), \quad (96)$$

where j is a prescribed function of m_{ϖ} . It is also worth noting that, by making use of the integral representation for the gravitational potential boundary conditions are automatically satisfied. The approximation scheme can now be viewed as follows. By using equation 96, a suitably chosen trial density distribution $\rho_o(\varpi, z)$ provides a function $\Phi_o(\varpi, z)$. This function, in turn, leads to an improved density distribution $\rho_1(\varpi, z)$ when equation 95 is taken into account. Similarly, when fed back into equation 96 this new function leads to an improved potential $\Phi_1(\varpi, z)$, etc. Thus, alternately solving equations 96 and 95, as exactly as numerical techniques permit, we eventually obtain a self-consistent solution by this iterative method. The method works remarkably well. According to Ostriker and Mark, for slowly rotating stars between ten or twenty iterations suffice to give excellent accuracy.

On the practical side, let us now briefly discuss the main steps of the numerical integration. It is apparent from equation 5 that given an explicit $p - \rho$ relation, equation 95 relates ρ and Φ through an algebraic operator. Hence, equilibrium step 95 in the iterative process is straightforward. On the other hand, the potential step 96 requires a numerical discretization of two integral operators that we will now discuss.

Suppose that the density $\rho(\varpi, z)$ is known at some step in the iterative scheme. Naturally, that function vanishes on a boundary that is not spherical and, in extreme cases, may be quite far from spheroidal. Expand now the density in appropriate polynomial form. It is convenient to define this expansion within a sphere of radius R centered about the center of mass of the configuration. We have

$$\rho(x, \mu) \cong \frac{3M}{4\pi R^3} \sum_{l=1}^N \sum_{m=l}^N A_{lm} x^{2m-2} P_{2l-2}(\mu), \quad (97)$$

where $x = r/R$ and $\mu = \cos\theta$. Let us note that we use only even-order Legendre polynomials because of the symmetry about the equatorial plane. Correspondingly, since we expand in the range $0 \leq x \leq 1$, only even powers of the radial coordinate need appear. Moreover, the constants A_{lm} must vanish if $m < l$ in order to maintain continuity at the origin. This first constraint also implies that the density assumes a finite value at the center of mass. In addition, although the true density vanishes on the circumscribed sphere, the approximate density does not vanish identically there. Thus, in order to minimize this error, we must add the constraint $\rho(1, \mu) = 0$. Finally, the parameter N , which determines the number of terms taken in the expansion, is chosen to give the requisite accuracy consistent with the limitations of time and storage capacity of the computer.

If we make use of equations 12-16, the gravitational potential 93 becomes

$$V(x, \mu) = -2\pi R^2 G \sum_{n=0}^{\infty} P_n(\mu) \int_{-1}^{+1} d\mu' P_n(\mu') \left(\int_0^x dx' \frac{x'^n}{x^{n+1}} + \int_x^1 dx' \frac{x'^n}{x'^{n+1}} \right) \rho(x', \mu') x'^2 \quad (98)$$

Substituting equation 97 into the foregoing expansion and integrating over μ' and x' we find

$$V(x, \mu) \cong -\frac{3}{2} \frac{GM}{R} \sum_{l=1}^N \sum_{m=l}^N \frac{A_{lm} P_{2l-2}(\mu)}{(m-l+1)(4l-3)} \left(x^{2l-2} - \frac{4l-3}{2m+2l-1} x^{2m} \right). \quad (99)$$

Thus, for any trial density (i.e. any given matrix A_{lm}), the gravitational potential can be derived at once. Similarly, for a prescribed function $j(m_{\varpi})$, we can thence express the centrifugal potential per unit mass 93 as a polynomial in the normalized variable ϖ/R . As in equations 97 and 99, the density occurs via the matrix A_{lm} . To summarize, given a trial density, we can find the total potential Φ in analytical form. The next step in the iterative process consists of substituting this potential into equation 95 and determining a new density.

This method has been extensively used to describe polytropes and zero-temperature white dwarfs in rapid differential rotation.

3.2 The HSCF Method

The SCF method is extremely effective, however, it failed to give solution for the case of high degree of flatness, i.e. for cases with $T/|W| > 0.25$. here T is the total rotational kinetic energy, and W the total potential energy. Moreover, for the case of high density contrast, it does not work well either, because the iteration does not converge. Of course, other methods, remarkably accurate, have been devised. Nevertheless, their excellent efficiency is strictly bound with very fast computing systems having large memory and storage capacities. The most popular is the one developed by Eriguchi and Müller, named Straightforward Newton-Raphson, abbreviated by SFNR. In the SFNR method, however a very dense 600x600 matrix must be inverted. One cannot find facilities even today when one wants to apply this method to a three-dimensional model.

In this work, we will present the method devised by Izumi Hachisu, which is as powerful as the SFNR method but much more efficient and much faster than the SFNR method for most cases. Although this method seems to be a variant of the SCF method, it has no limitations, in contrast with the original version. In order to demonstrate the power of this method we have computed several models of polytropic neutron stars. This method can also be applied to the case of fully degenerate white dwarfs. We only mention this case, without any further detailed numerical calculations.

3.2.1 Formulation of Basic Equations and Assumptions.

At this point we repeat the basic assumptions made in §2.2 and §2.7:

- (i) *the star is isolated in space and rotates about a fixed axis with some yet unspecified angular velocity*
- (ii) *the system is stationary when viewed in an inertial frame of reference, and the density of each mass element remains a constant as we follow its motion*
- (iii) *friction may be neglected altogether*
- (iv) *no electromagnetic force is acting upon the star*
- (v) *the geometry of the problem is axisymmetric*
- (vi) *the angular velocity is a function of the distance $\varpi = r(1 - \mu^2)^{1/2}$*
- (vii) *the EOS is barotropic i.e. the pressure P is solely a function of the density ρ*

a) Integral Representation of Basic Equations

According to the aforementioned assumptions the equation governing the equilibrium is the integral of motion, which was proved in §2.7

$$\int \rho^{-1} dP + \Phi - \int \Omega^2 \varpi d\varpi = C(\text{constant}), \quad (100)$$

where we use spherical coordinates (r, μ, ϕ) , r being the distance from the center of mass, μ the cosine of the angle θ from the axis of rotation, ϕ the azimuthal angle from the x -axis and Φ the gravitational potential. Here we employ an integral representation for it is easier to handle the boundary conditions. The symmetry about the equatorial plane is valid according to the Lichtenstein theorem. Then the gravitational potential can be calculated from ⁷

$$\begin{aligned} \Phi(\mathbf{r}) &= -G \int \frac{\rho(\mathbf{r}')}{|\mathbf{r} - \mathbf{r}'|} d^3\mathbf{r}' = \\ &= -4\pi G \int_0^\infty dr' \int d\mu' \sum_{n=0}^\infty f_{2n}(r', r) P_{2n}(\mu) P_{2n}(\mu') \rho(\mu', r'), \end{aligned} \quad (101)$$

where

$$f_{2n}(r', r) = \begin{cases} \frac{r'^{2n+2}}{r^{2n+1}}, & \text{if } r' < r, \\ \frac{r^{2n}}{r'^{2n-1}}, & \text{if } r' > r. \end{cases} \quad (102)$$

⁷For a detailed discussion on expansion in Legendre polynomials and Green functions cf. [6, sel. 95-127]

b) *Equation of State*

In this work we will use two types of EOS. The first one is the polytropic EOS

$$P = K\rho^{1+1/N}, \quad (103)$$

where N is called the polytropic index and K the polytropic constant. The first term of equation 100 can be integrated analytically, thus obtaining

$$\int \rho^{-1} dP = (1 + N) \frac{P}{\rho} \stackrel{(103)}{=} (1 + N) K \rho^{1/N} \quad (104)$$

The second type of EOS is that of zero-temperature white dwarf, i.e.

$$\begin{aligned} P &= \alpha [x(2x^2 - 3)(x^2 + 1)^{1/2} + 3 \sinh^{-1} x], \\ \rho &= bx^3, \end{aligned} \quad (105)$$

where $\alpha = 6.00x10^{22} \text{ dynes}\cdot\text{cm}^{-2}$ and $b = 9.82x10^5 \mu_e \text{ g}\cdot\text{cm}^{-3}$. Here the mean molecular weight μ_e is fixed at 2. The choice of α, b and μ_e corresponds to the case in which the Chandrasekhar mass is $1.44M_\odot$. For the white dwarf case the first term in equation 100 can be integrated, thus finding

$$\int \rho^{-1} dP = \frac{8\alpha}{b} \left[1 + \frac{\rho^{2/3}}{b} \right]^{1/2}. \quad (106)$$

The quantity in equation 104 or equation 106 is usually called *enthalpy* and is denoted by H . Then equation 100 becomes

$$H = C - \Phi + \int \Omega^2 \varpi d\varpi, \quad (107)$$

where the constant value C is determined to satisfy the boundary conditions, which will be mentioned later. The density is related to H from equation 104

$$\rho = \frac{H}{K(N + 1)} \quad (108)$$

for polytropic stars, and from equation 106

$$\rho = b \left[\left(\frac{bH}{8\alpha} \right)^2 - 1 \right]^{3/2} \quad (109)$$

for the white dwarf. These two expressions will be used successively to obtain new density distributions in the iteration process of the self-consistent field method. The method itself will be described later.

g) *Rotation Laws*

Two types of rotation law will be considered: rigid and v -constant rotation. In each case the squared angular velocity Ω^2 can be expressed as follows

(i) rigid rotation:

$$\Omega^2 = \Omega_0^2 \quad (= \text{constant}), \quad (110)$$

(ii) v -constant rotation:

$$\Omega^2 = \frac{v_0^2}{d^2 + \varpi^2}, \quad (111)$$

where d is an arbitrary parameter. As d decreases towards zero, the rotation law expressed by equation 111, tends to the true rotation as indicated by its name, i.e., where the rotational velocity v_ϕ is strictly constant in space.

For these two cases, the third term in equation 100 can be integrated analytically, and we have the following generalized form:

$$- \int \Omega^2 \varpi d\varpi = h_0^2 \Psi(\varpi), \quad (112)$$

where

$$\Psi(\varpi) = \begin{cases} -\varpi^2/2, & (\text{rigid}) \\ -(1/2) \ln(1 + \frac{\varpi^2}{d^2}), & (v\text{-constant}) \end{cases} \quad (113)$$

and

$$h_0^2 = \begin{cases} \Omega_0^2, & (\text{rigid}) \\ v_0^2, & (v\text{-constant}) \end{cases} \quad (114)$$

Then equation 107 can be written as follows

$$H = C - \Phi - h_0^2 \Psi(\varpi) \quad (115)$$

3.2.2 Plan of the Method

We still have not understood the reason why the original SCF method failed to give very distorted configurations although they are equilibrium figures. Nevertheless, we will consider a way to compute very distorted configurations and we will use basically almost the same iteration scheme as that of the SCF method. The iteration procedure itself goes as follows: The gravitational potential is calculated from the given density distribution, by making use of equation 101. The enthalpy, which is obtained from equation 115, can be related to the density distribution through equation 108 for the polytropic case, or equation 109 for the white dwarf case. This new density distribution is used as the given density distribution in the next iteration step. We repeat this iteration procedure until the relative difference between two consecutive iteration steps becomes sufficiently small. The final density distribution can be considered to obtain self-consistency.

First we should try to find out what the essential factor is in the successful method SFNR. In this method, the iteration procedure was performed by fixing one special parameter, *the axis ratio*. This parameter determines the equilibrium uniquely. The most important point is to decide what parameter we choose. Here, we will use the axis ratio as in SFNR. Since the configuration is equatorially symmetric, two points, A and B, determine the axis ratio uniquely, as seen in figure 3. We set point A on the equatorial surface. On the other hand, point B is set on the z -axis (the axis of rotation) for a spheroidal configuration, or on the equatorial plane ($x - y$ plane) for an annular configuration.

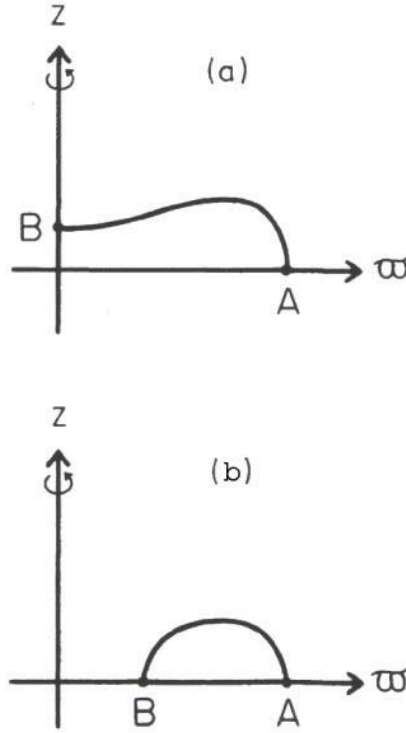


Figure 3: Two points on the boundary surface, determine uniquely a stellar model : (a) spheroidal structure, (b) toroidal structure.

Second, we must choose a basis of dimensional variables which consists of three quantities, in order to make all variables dimensionless. We employ this for three reasons: a) Dimensionless variables can very easily be converted to whatever system of units one may desire, b) many programming languages have generic problems when dealing with exceedingly large number. Therefore, dividing one's numerical results by a convenient weight parameter, one can reduce the size of these figures by many orders of magnitude, g) it is much easier to compare our results with with similar results, which already exist in international literature. We adopt the maximum density ρ_{max} , the equatorial radius $R_e (= r_A$, the radius at point A), and the constant of gravity G , instead of the total mass M , the total angular momentum J and the maximum radius of the surface R_{max} , which have been used in the past by other researchers. It is very important to choose ρ_{max} as one of the parameters in order to achieve numerically stable equilibrium. Otherwise, the density vanishes during the iteration procedure. We may use the total mass M instead, but this selection requires a more complicated treatment. In general, the maximum density is not attained at the center, for a ring structure or a pear-shaped structure appears for the case of large angular momentum. So, we have not used the central density, which was adopted by many authors in the past.

a) *Boundary Conditions*

On the surface of the star, both the density and the pressure vanish. Therefore, the boundary condition on the surface is given by

$$H = 0 \tag{116}$$

for polytropic stars and

$$x = 0 \left(\eta' H = \frac{8\alpha}{b} \right) \tag{117}$$

for the white dwarfs. First, we consider the polytropic case. The values of H vanish at two boundary points A and B as mentioned above. Hence, the boundary condition 116 is:

$$H(A) = 0 = C - \Phi(A) - h_0^2 \Psi(A), \tag{118}$$

$$H(B) = 0 = C - \Phi(B) - h_0^2 \Psi(B). \tag{119}$$

These expressions can be rewritten as follows

$$h_0^2 = - \frac{\Phi(A) - \Phi(B)}{\Psi(A) - \Psi(B)}, \tag{120}$$

$$C = \Phi(A) + h_0^2 \Psi(A). \tag{121}$$

These relations will be used to determine the coefficient h_0^2 and the constant C during the iteration procedure, because we fix two points, A and B, and then we have to calculate the foregoing parameters to know enthalpy H.

Next, we have the boundary conditions for the white dwarf case as follows

$$H(A) = \frac{8\alpha}{b} = C - \Phi(A) - h_0^2 \Psi(A), \tag{122}$$

$$H(B) = \frac{8\alpha}{b} = C - \Phi(B) - h_0^2 \Psi(B). \tag{123}$$

and the same expressions as in equations 120 and 121 are obtained, i.e.

$$h_0^2 = - \frac{\Phi(A) - \Phi(B)}{\Psi(A) - \Psi(B)}, \tag{124}$$

$$C = \frac{8\alpha}{b} + \Phi(A) + h_0^2 \Psi(A). \tag{125}$$

b) *Iteration Procedure*

At the first step of the iteration procedure we must provide a trial density distribution, i.e., ⁸, ρ_n (where n is the iteration number and $n = 0$ for the initial guess). The gravitational potential Φ_n can be calculated for this density distribution through equation 101. Then, given the rotation law, we can obtain $h_{0,n}^2$ from equation 120 for the polytropes or from equation 124 for the white dwarfs. After calculating C_n from equation 121 for the polytropic case or equation 125

⁸In this work we provide as a trial density distribution, the one obtained by the model of the stationary Newtonian star. cf. appendix B

for the white dwarf case, we are bale to calculate the enthalpy H_n by making use of equation 115. A new density distribution ρ_{n+1} can be calculated using equation 108 for the polytropes or equation 109 for the white dwarfs. These procedure will be repeated until all the absolute values of three relative differences

$$\frac{(H_{n+1} - H_n)_{max}}{H_{n+1,max}}, \quad \frac{h_{0,n+1} - h_{0,n}}{h_{0,n+1}} \kappa_{\alpha\iota} \quad \frac{C_{n+1} - C_n}{C_{n+1}} \quad (126)$$

become smaller than a small value δ . In the present work, we adopt $\delta = 10^{-4}$. Here, the subscript ‘‘max’’ denotes the maximum value of the corresponding variable.

c) Dimensionless Variables

We introduce a dimensionless form of the physical variables. The basis for a set of dimensionless variables consists of three quantities: the maximum density ρ_{max} , the equatorial radius of the surface R_e and the gravitational constant G , as mentioned above. For simplicity, we will use the same notation as for the dimensional variables, but the dimensionless variables will be indicated by a carte when we must distinguish them from the dimensional ones. On this basis, dimensionless variables are defined as follows

$$\hat{\rho} = \frac{\rho}{\rho_{max}} \quad (127)$$

$$\hat{\varpi} = \frac{\varpi}{R_e} \quad (128)$$

$$\hat{r} = \frac{r}{R_e} \quad (129)$$

$$\hat{d} = \frac{d}{R_e} \quad (130)$$

$$\hat{\Phi} = \frac{\Phi}{GR_e^2 \rho_{max}} \quad (131)$$

$$\hat{P} = \frac{P}{GR_e^2 \rho_{max}^2} \quad (132)$$

$$\hat{\Omega}^2 = \frac{\Omega^2}{G \rho_{max}} \quad (133)$$

$$\hat{H} = \frac{H}{GR_e^2 \rho_{max}} \quad (134)$$

$$\hat{C} = \frac{C}{GR_e^2 \rho_{max}} \quad (135)$$

and other variables can be calculated from these transformations. For example, the total mass M , the total angular momentum J , the gravitational potential energy W , the]rotational kinetic energy T and the moment of inertia I are normalized as follows

$$\hat{M} = \frac{M}{R_e^3 \rho_{max}} \quad (136)$$

$$\hat{J} = \frac{J}{G^{1/2} R_e^5 \rho_{max}^{3/2}} \quad (137)$$

$$\hat{W} = \frac{W}{GR_e^5 \rho_{max}^2} \quad (138)$$

$$\hat{T} = \frac{T}{GR_e^5 \rho_{max}^2} \quad (139)$$

$$\hat{I} = \frac{I}{R_e^5 \rho_{max}} \quad (140)$$

d) *Dimensionless Form of Basic Relations*

The real computation is performed in the dimensionless form. When ρ_{max} , is given the radius R_e at the equator can be calculated as follows: if we substitute the dimensionless form of the variables ρ, H into equations 108 and 109 and take into account, that when $\rho = \rho_{max} \Rightarrow H = H_{max} \Rightarrow \hat{H} = \hat{H}_{max}$ then, if solve the resultant equation with respect to the equatorial surface radius, we obtain:

$$R_e = \left[K(1+N) \frac{\rho_{max}^{-1+1/N}}{G \hat{H}_{max}} \right]^{1/2} \quad (141)$$

for the polytropic star case and

$$R_e = \left[\frac{8\alpha(1+x_{max}^2)^{1/2}}{bG\rho_{max}\hat{H}_{max}} \right]^{1/2} \quad (142)$$

for the white dwarf case.

Substituting the dimensionless form of physical variables, we find that the dimensionless density can be derived from the dimensionless enthalpy by making use of the following equation

$$\hat{\rho} = \begin{cases} \left(\frac{\hat{H}}{\hat{H}_{max}} \right)^N, & \hat{H} \geq 0 \\ 0, & \hat{H} < 0 \end{cases} \quad (143)$$

for the polytropic case

$$\hat{\rho} = \left(\frac{x}{x_{max}} \right)^3 \quad (144)$$

where x is a parameter defined by

$$x = \begin{cases} \left[\max \left\{ (1+x_{max}^2) \left(\frac{\hat{H}}{\hat{H}_{max}} \right)^2 - 1, 0 \right\} \right]^{1/2}, & \hat{H} \geq 0 \\ 0, & \hat{H} < 0 \end{cases} \quad (145)$$

and

$$x_{max} = \left(\frac{\rho_{max}}{b} \right)^{1/3} \quad (146)$$

for the white dwarf case. Here, \hat{H}_{max} is the maximum value of \hat{H} .

For example we give the calculation of the dimensionless form of equation 101. If we use spherical coordinates equation 101 can be written as follows

$$\Phi = -G \int \frac{\rho(\mathbf{r}')}{|\mathbf{r} - \mathbf{r}'|} r'^2 \sin^2 \theta' dr' d\theta' d\phi' \hat{\mathbf{r}}', \quad (147)$$

where $\hat{\mathbf{r}}'$ is the unit vector along the direction of vector \mathbf{r}' . We substitute Φ, ρ, r from equations 131, 127 and 129 into the former equation, thus obtaining

$$\hat{\Phi} \cdot GR_e^2 \rho_{max} = -G \int \frac{\hat{\rho} \cdot \rho_{max} \hat{r}'^2}{|\hat{\mathbf{r}} - \hat{\mathbf{r}}'| R_e} \cdot R_e^2 \sin \theta' d\hat{r}' \cdot R_e d\theta' d\phi' \hat{\mathbf{r}}' \quad (148)$$

after cancelling the same terms and expanding in Legendre Polynomials we find

$$\hat{\Phi} = - \int \frac{\hat{\rho}(\hat{\mathbf{r}}')}{|\hat{\mathbf{r}} - \hat{\mathbf{r}}'|} d^3 \hat{\mathbf{r}}' \quad (149)$$

$$= -4\pi \int_0^\infty d\hat{r}' \int_0^1 d\mu' \sum_{n=0}^\infty f_{2n}(\hat{r}', \hat{r}) P_{2n}(\mu) P_{2n}(\mu') \hat{\rho}(\mu', \hat{r}'), \quad (150)$$

where

$$f_{2n}(\hat{r}', \hat{r}) = \begin{cases} \frac{\hat{r}'^{2n+2}}{\hat{r}^{2n+1}}, & \text{if } \hat{r}' < \hat{r}, \\ \frac{\hat{r}^{2n}}{\hat{r}'^{2n-1}}, & \text{if } \hat{r}' > \hat{r}. \end{cases} \quad (151)$$

We summarize the method. The dimensionless gravitational potential can be calculated from the given density distribution by virtue of equation 150 for both the polytropic and zero-temperature white dwarf case. Next, we calculate \hat{h}_0^2 and \hat{C} from the boundary conditions using the dimensionless form of equations 120 and 121 for the polytropes, i.e.

$$\hat{h}_0^2 = - \frac{\hat{\Phi}(A) - \hat{\Phi}(B)}{\hat{\Psi}(A) - \hat{\Psi}(B)}, \quad (152)$$

$$\hat{C} = \hat{\Phi}(A) + \hat{h}_0^2 \hat{\Psi}(A). \quad (153)$$

For the white dwarf case we calculate \hat{h}_0^2 and \hat{C} by making use of

$$\hat{h}_0^2 = - \frac{\hat{\Phi}(A) - \hat{\Phi}(B)}{\hat{\Psi}(A) - \hat{\Psi}(B)}, \quad (154)$$

$$\hat{C} = \frac{\hat{H}_{max}}{(1 + x_{max}^2)^{1/2}} + \hat{\Phi}(A) + \hat{h}_0^2 \hat{\Psi}(A). \quad (155)$$

where we have used the relation $8\hat{\alpha}/\hat{b} = \hat{H}_{max}/(1 + x_{max}^2)^{1/2}$ which is derived by equation 142 and the requirement that $8\hat{\alpha}/\hat{b} = 8\alpha/bGR_e^2\rho_{max}$. This last requirement can be easily understood if we take into account that α/b has enthalpy units, a fact derived by equation 122. Therefore, it must be normalized the same way as the enthalpy does. We define now, a new variable, which does not include the constant \hat{C} :

$$\hat{F} = \hat{H} - \hat{C} = -\hat{\Phi} - \hat{h}_0^2 \hat{\Psi}(\hat{r}) \quad (156)$$

It is noted that two variables \hat{H} and \hat{F} have maximum values at the same point. The maximum value of \hat{F} is denoted by \hat{F}_{max} . After replacing \hat{H} in equation 155 with $\hat{F} + \hat{C}$ we have

$$\hat{C} = \frac{\hat{F}_{max} - (1 + x_{max}^2)^{1/2} \hat{F}(A)}{(1 + x_{max}^2)^{1/2} - 1}. \quad (157)$$

In the real calculation, we use equations 152 and 153 for the polytropic stars, and equations 154 and 157 for the white dwarfs.

3.2.3 Numerical Technique

a) Discretization

The total mesh number is $KDIV \times NDIV$, where $KDIV$ is the mesh number in the μ -direction and $NDIV$ the mesh number in the r -direction. Usually it is 129×129 or 257×257 . Each direction is divided into equal mesh intervals, i.e.

$$r_j = r_{max} \frac{j-1}{NDIV-1}, \quad j = 1, \dots, NDIV \quad (158)$$

$$\mu_i = \frac{i-1}{KDIV-1}, \quad i = 1, \dots, KDIV \quad (159)$$

where r_{max} is to be somewhat larger than unity, for the maximum radius may be attained off the equatorial plane. In the present work $r_{max} = 16/15$ is equal to $16/15$.

Physical variables are evaluated at the cross point of two mesh lines, i.e.

$$\rho_{i,j} = \rho(\mu_i, r_j), \quad (160)$$

$$\Phi_{i,j} = \Phi(\mu_i, r_j), \quad (161)$$

and so on.

b) Numerical Integration

To maintain second-order accuracy, we integrate equation 150 by virtue of Simpson's three-point formula. That is why the mesh number in each direction is odd. Then the gravitational potential is calculated in three steps:

$$D_{k,n}^{(1)} = \sum_{i=1(2)}^{KDIV-2} \frac{1}{6} (\mu_{i+2} - \mu_i) [P_{2n}(\mu_i) \hat{\rho}_{i,k} + 4P_{2n}(\mu_{i+1}) \hat{\rho}_{i+1,k} + P_{2n}(\mu_{i+2}) \hat{\rho}_{i+2,k}], \quad (162)$$

$$D_{n,j}^{(2)} = \sum_{k=1(2)}^{NDIV-2} \frac{1}{6} (\hat{r}_{k+2} - \hat{r}_k) \times \\ \times [f_{2n}(\hat{r}_k, \hat{r}_j) D_{k,n}^{(1)} + 4f_{2n}(\hat{r}_{k+1}, \hat{r}_j) D_{k+1,n}^{(1)} + f_{2n}(\hat{r}_{k+2}, \hat{r}_j) D_{k+2,n}^{(1)}], \quad (163)$$

$$\hat{\Phi}_{i,j} = -4\pi \sum_{n=0}^{LMAX} D_{n,j}^{(2)} P_{2n}(\mu_i), \quad (164)$$

where such notation as $i = 1(2)$ means that i increases by increments of 2, starting from 1. $LMAX$ denotes the cutoff number of Legendre polynomials used in this computation [usually $LMAX = 16$, i.e. up to $P_{32}(\mu)$], and as mentioned earlier both $NDIV$ and $KDIV$ are odd numbers. Since the mesh (μ_i, r_j) is fixed during the calculation, we compute $f_{2n}(r_k, r_j)$ and $P_{2n}(\mu_i)$ at the beginning of the whole procedure. These techniques help speed up the computation, since the calculation of the gravitational potential needs the most lengthy computer time.

Other integrated values, such as M and W , are also calculated in the same way as the gravitational potential is

$$Q_j^{(1)} = \sum_{i=1(2)}^{KDIV-2} \frac{1}{6} (\mu_{i+2} - \mu_i) [\hat{\rho}_{i,j} + 4\hat{\rho}_{i+1,j} + \hat{\rho}_{i+2,j}], \quad (165)$$

$$M = 4\pi \sum_{j=1(2)}^{NDIV-2} \frac{1}{6} (\hat{r}_{j+2} - \hat{r}_j) [\hat{r}_j^2 Q_j^{(1)} + 4\hat{r}_{j+1}^2 Q_{j+1}^{(1)} + \hat{r}_{j+2}^2 Q_{j+2}^{(1)}], \quad (166)$$

$$S_j^{(1)} = \sum_{i=1(2)}^{KDIV-2} \frac{1}{6} (\mu_{i+2} - \mu_i) [\hat{\rho}_{i,j} \hat{\Phi}_{i,j} + 4\hat{\rho}_{i+1,j} \hat{\Phi}_{i+1,j} + \hat{\rho}_{i+2,j} \hat{\Phi}_{i+2,j}], \quad (167)$$

$$W = -2\pi \sum_{j=1(2)}^{NDIV-2} \frac{1}{6} (\hat{r}_{j+2} - \hat{r}_j) [\hat{r}_j^2 S_j^{(1)} + 4\hat{r}_{j+1}^2 S_{j+1}^{(1)} + \hat{r}_{j+2}^2 S_{j+2}^{(1)}], \quad (168)$$

At this point, we will present how we derive such discretized relations. As an example, we will obtain similar relations for both the rotational kinetic energy and the total angular momentum.

For the general case of differential rotation the norm of the angular momentum ⁹ is given by

$$\begin{aligned} J &= \int (|\vec{r} \times \vec{v}| dm) \\ &= \left(\int r v_\phi \rho(\mu, r) d^3 r \right) |\hat{e}_z| \\ &= \int r \Omega(\mu, r) \varpi \rho(\mu, r) r^2 dr d\phi d\mu \\ &= 2\pi \int_0^\infty \int_{-1}^1 r^3 \Omega(\mu, r) r (1 - \mu^2)^{1/2} \rho(\mu, r) d\mu dr \Rightarrow \\ J &= 4\pi \int_0^\infty \left(\int_0^1 \Omega(\mu, r) \rho(\mu, r) (1 - \mu^2)^{1/2} d\mu \right) r^4 dr \end{aligned} \quad (169)$$

In equation 169 we have to calculate two integrals by using the three-point Simpson's formula. We have

$$Q_j^{(2)} = \sum_{i=1(2)}^{KDIV-2} \frac{1}{6} (\mu_{i+2} - \mu_i) [\hat{\Omega}_{i,j} \hat{\rho}_{i,j} (1 - \mu_i^2)^{1/2} + 4\hat{\Omega}_{i+1,j} \hat{\rho}_{i+1,j} (1 - \mu_{i+1}^2)^{1/2} + \hat{\Omega}_{i+2,j} \hat{\rho}_{i+2,j} (1 - \mu_{i+2}^2)^{1/2}], \quad (170)$$

$$J = 4\pi \sum_{j=1(2)}^{NDIV-2} \frac{1}{6} (\hat{r}_{j+2} - \hat{r}_j) [\hat{r}_j^4 Q_j^{(2)} + 4\hat{r}_{j+1}^4 Q_{j+1}^{(2)} + \hat{r}_{j+2}^4 Q_{j+2}^{(2)}], \quad (171)$$

The rotational kinetic energy is given by

$$T = \frac{1}{2} \int \Omega dJ \quad (172)$$

⁹It can easily be proved that in the dimensionless form we have adopt, the definition of the angular momentum remains the same. That is why we use dimensionless variables in its discretized form.

If we take into consideration equation 169, we found for the rotational kinetic energy in the case of axisymmetrical differential rotation

$$T = 4\pi \int_0^\infty \left(\int_0^1 \Omega^2(\mu, r) \rho(\mu, r) (1 - \mu^2)^{1/2} d\mu \right) r^4 dr \quad (173)$$

the numerical integration of this last equation gives

$$S_j^{(2)} = \sum_{i=1(2)}^{KDIV-2} \frac{1}{6} (\mu_{i+2} - \mu_i) [\hat{\Omega}_{i,j}^2 \hat{\rho}_{i,j} (1 - \mu_i^2)^{1/2} + 4\hat{\Omega}_{i+1,j}^2 \hat{\rho}_{i+1,j} (1 - \mu_{i+1}^2)^{1/2} + \hat{\Omega}_{i+2,j}^2 \hat{\rho}_{i+2,j} (1 - \mu_{i+2}^2)^{1/2}], \quad (174)$$

$$J = 2\pi \sum_{j=1(2)}^{NDIV-2} \frac{1}{6} (\hat{r}_{j+2} - \hat{r}_j) [\hat{r}_j^4 S_j^{(2)} + 4\hat{r}_{j+1}^4 S_{j+1}^{(2)} + \hat{r}_{j+2}^4 S_{j+2}^{(2)}], \quad (175)$$

For the case, in which the star rotates as a rigid body the rotational kinetic energy is given by

$$T = \frac{1}{2} I \Omega_o^2 \quad (176)$$

where Ω_o is the constant angular velocity. On the other hand, the star's moment of inertia is given by

$$I = \int \varpi^2 dm = \int r^2 (1 - \mu^2) \rho(\mu, r) d^3r = 4\pi \int_0^\infty \left(\int_0^1 \rho(\mu, r) (1 - \mu^2) d\mu \right) r^4 dr \quad (177)$$

Integrating this by virtue of Simposn's formula, we obtain

$$G_j^{(2)} = \sum_{i=1(2)}^{KDIV-2} \frac{1}{6} (\mu_{i+2} - \mu_i) [\hat{\rho}_{i,j} (1 - \mu_i^2) + 4\hat{\rho}_{i+1,j} (1 - \mu_{i+1}^2) + \hat{\rho}_{i+2,j} (1 - \mu_{i+2}^2)], \quad (178)$$

$$I = 4\pi \sum_{j=1(2)}^{NDIV-2} \frac{1}{6} (\hat{r}_{j+2} - \hat{r}_j) [\hat{r}_j^4 G_j^{(2)} + 4\hat{r}_{j+1}^4 G_{j+1}^{(2)} + \hat{r}_{j+2}^4 G_{j+2}^{(2)}], \quad (179)$$

Unlike in the previous integrals, where the vanishing of the density defines the surface of the star, when we calculate the volume, we need to have prior knowledge of the surface. Thus, for every direction μ we calculate the distance $r_{bound}(\mu)$ where the enthalpy goes through zero. In fact, we first find the two mesh points where the enthalpy changes sign and then use linear interpolation to find a better value for the position of the boundary. One could also use higher order interpolation, but since the mesh is fine enough, the introduced error is very small. The volume is then calculated by

$$\begin{aligned} V &= \int d^3r \\ &= 4\pi \int_0^1 \left(\int_0^{r_{bound}} r^2 dr \right) d\mu \Rightarrow \\ V &= \frac{4\pi}{3} \int_0^1 r_{bound}^3(\mu) d\mu \end{aligned} \quad (180)$$

By applying Simpson's formula for the calculation of this last integral, we find

$$V = \frac{4\pi}{3} \sum_{i=1(2)}^{KDIV-2} \frac{1}{6} (\mu_{i+2} - \mu_i) (r_{bound,i}^3 + 4r_{bound,i+1}^3 + r_{bound,i+2}^3) \quad (181)$$

For the calculation of $r_{bound,i}$ we use the first-order asymptotic Lagrange polynomial.

$$P_1(r) = \frac{r - r_2}{r_1 - r_2} H_1 + \frac{r - r_1}{r_2 - r_1} H_2 \quad (182)$$

where r_1, r_2 denote arbitrary points at which the enthalpy changes sign, with H_1 being its positive value and H_2 its negative one. If we set $P_1(r)$ equal to zero (since the enthalpy must vanish) and solve with respect to r , we obtain the numerical relation from which we derive $r_{bound,i}$

$$r = \frac{r_2 H_1 - r_1 H_2}{H_1 - H_2} \quad (183)$$

b) Numerical Accuracy Check

The accuracy of the numerical solutions have been evaluated by the virial relation. We introduce

$$VC = \frac{|2T + W + 3\Pi|}{|W|}, \quad (184)$$

where P is the volume integral of pressure, i.e.

$$\Pi = \int P d^3\mathbf{r}. \quad (185)$$

Its dimensionless form is numerically calculated by

$$G_j^{(1)} = \sum_{i=1(2)}^{KDIV-2} \frac{1}{6} (\mu_{i+2} - \mu_i) [\hat{P}_{i,j} + 4\hat{P}_{i+1,j} + \hat{P}_{i+2,j}], \quad (186)$$

$$\hat{\Pi} = 4\pi \sum_{j=1(2)}^{NDIV-2} \frac{1}{6} (\hat{r}_{j+2} - \hat{r}_j) [\hat{r}_j^2 G_j^{(1)} + 4\hat{r}_{j+1}^2 G_{j+1}^{(1)} + \hat{r}_{j+2}^2 G_{j+2}^{(1)}], \quad (187)$$

where

$$\hat{\Pi} = \frac{\Pi}{GR_e^5 \rho_{max}^2} \quad (188)$$

It is considered that the relative accuracy of the numerical solution is of the same order as the value of VC . When VC is greater than 10^{-3} , the number of mesh points is increased until the value of VC becomes smaller than 10^{-3} . In the present project, VC is usually a few times 10^{-4} .

c) *Critical Rotation*

For both polytropic (except $N=0$) and realistic equations of state, there exists an axis ratio for which the angular velocity reaches the Keplerian limit

$$\Omega_K^2 = \frac{\Phi'}{R_e}, \quad (189)$$

where $' = \frac{d}{dr}$ and R_e is the equatorial radius of the surface. The dimensionless form of 189 is

$$\hat{\Omega}_K^2 = \hat{\Phi}'. \quad (190)$$

Further increase of the angular velocity results in matter shed out of the star from the equatorial region. Differentiating the equilibrium equation we obtain

$$\hat{\Phi}' = -\hat{H}' + \Omega_0^2 \hat{r}(1 - \mu^2). \quad (191)$$

Since at the equator $\mu = 0$ and $\hat{r} = r_A = 1$, by combining these two last equations we yield

$$\hat{\Omega}_K^2 = -\hat{H}' + \hat{\Omega}_0^2 \quad (192)$$

4 Numerical Results

4.1 Rigidly Rotating Neutron Stars

Six sequences of the polytropic index have been computed, i.e. $N=0, 0.1, 0.5, 1.5, 3.0$ and 4.0 .

First we summarize the results of $N=0$. The computation has been started from the spherical configuration: point B is set at $r_B = 1$ and $\mu_B = 1$ (point A is always set at $r_A = 1$ and $\mu_A = 0$). After obtaining the spherical model, we move point B down to the origin¹⁰ of the coordinate system along the z -axis step by step. It is noted that for each new model (i.e. each new position of point B) we use as a trial density at the first step of the iteration procedure, the self-consistent density, obtained in the calculation of the previous model. After point B has reached the origin, it is moved right towards point A, along the ϖ -axis, as seen in figure 3b. Solution at each step can be obtained easily after five or six iteration cycles.

The numerical results are summarized in Table 1. All physical variables listed in Table 1 are dimensionless. Here, r_B is the distance between the origin and point B. Point B is on the z -axis when r_B is positive (Fig. 3 a), while it is on the ϖ -axis when r_B is negative (Fig. 3 b). The volume is designated by V and P_{max} denotes the maximum pressure. The maximum value of the enthalpy H_{max} and the total internal energy U are not listed in Table 1, but they are easily calculated from

$$\hat{H}_{max} = (1 + N)\hat{P}_{max}, \quad (193)$$

$$\hat{U} = N\hat{\Pi}. \quad (194)$$

Figures 4,5,6 and 7 show the density distributions in the meridional plane. In fact, each of these figures show how the star's shape is like when viewed in the meridional plane. In these figures, the outer curve stands for the spherical model of the corresponding polytropic case (i.e the non-rotating star having the same polytropic index as that of the rotating star under consideration). As it is obvious from the results listed in Table I, different models have different masses and volumes and their shapes do not correspond to their realistic dimensions. We draw the spherical star as a measure of comparison between the rapidly rotating model and the stationary one.

In Table I we summarize the basic properties of the models, which we have computed. A first remark can be made. For each polytropic index, every model for which the axis ratio is equal to one, both the angular velocity and the angular momentum, as well as the rotational kinetic energy vanish. This result was anticipated, for only stationary models can assume spherical symmetry. Moreover, these models have equal volumes for their dimensionless radius is always equal to unity. However, their density distributions differ due to the different EOS, ergo their other properties differ either. Our results are generally in good agreement with those obtained by Izumi Hachisu, except for the highly flattened models. This is because, we have done our calculations using a (193×193) grid, which is smaller than that, which Hachisu used.

¹⁰In the present work we always set point B on a mesh point.

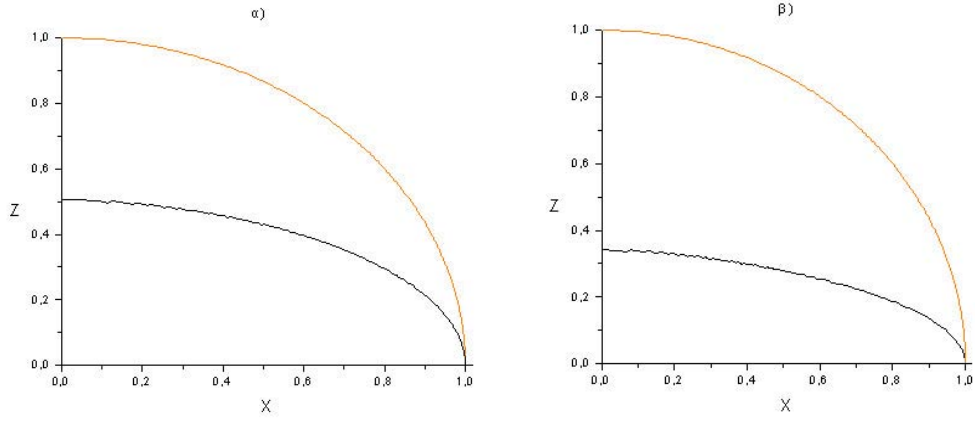


Figure 4: Meridional profile of rotating neutron stars with polytropic index $N=0.0$: (a) axis ratio $r_B = 0.5$, (b) axis ratio $r_B = 0.333$.

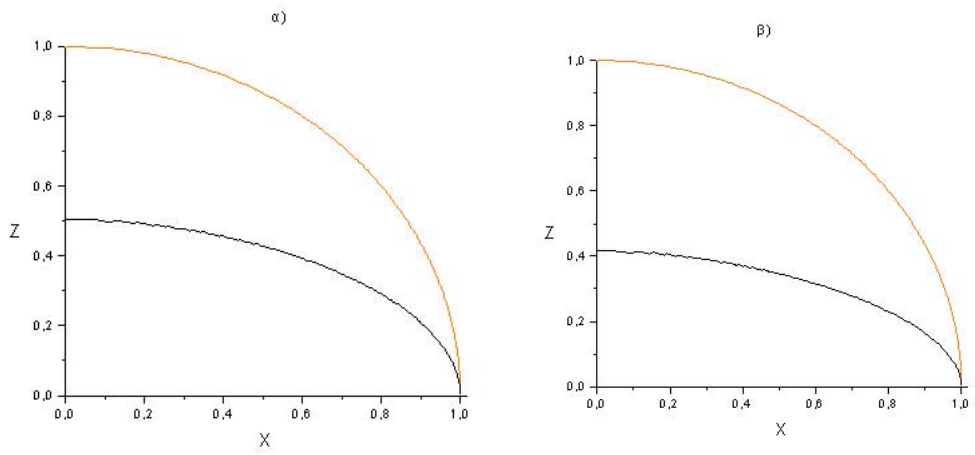


Figure 5: Meridional profile of rotating neutron stars with polytropic index $N=0.1$: (a) axis ratio $r_B = 0.5$, (b) axis ratio $r_B = 0.411$.

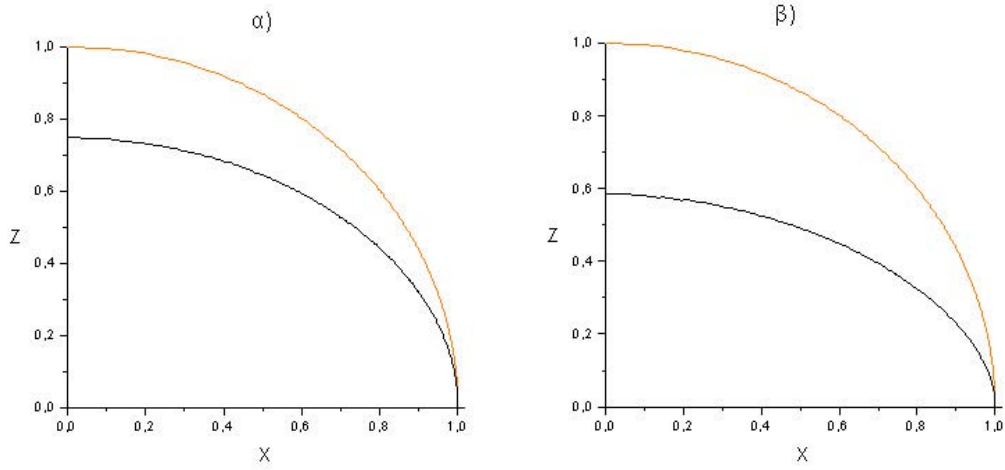


Figure 6: Meridional profile of rotating neutron stars with polytropic index $N=0.5$: (a) axis ratio $r_B = 0.748$, (b) axis ratio $r_B = 0.581$.

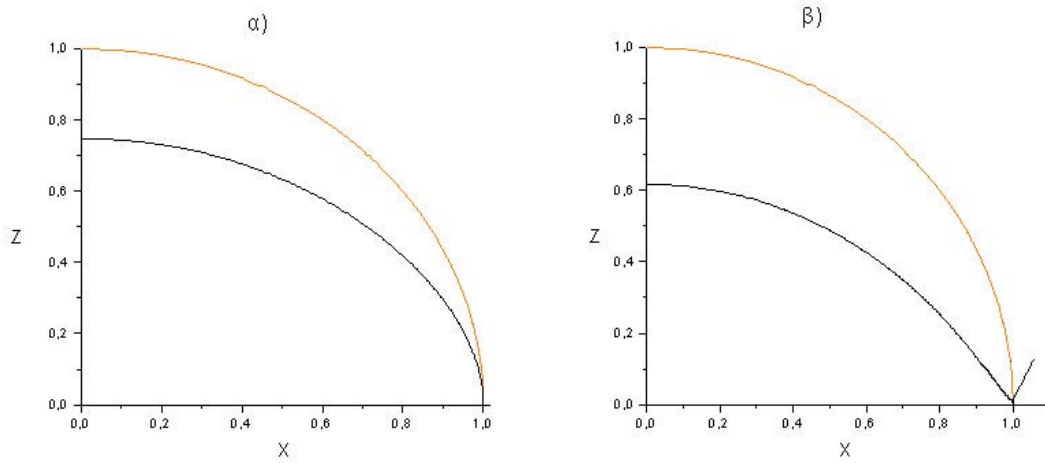


Figure 7: Meridional profile of rotating neutron stars with polytropic index $N=1.5$: (a) axis ratio $r_B = 0.75$, (b) axis ratio $r_B = 0.625$, this is a critical rotation case.

TABLE I
Rigid Rotation

r_B	$O_{\{0\}}^2$	M	V	J	T	-W	3Pi	Pmax
N=0.0								
1.000	0.000	4.17	4.18	0.000	0.000	10.47	10.77	2.187
0.500	1.369	2.07	2.07	0.924	0.540	3.163	2.112	0.892
0.333	1.460	1.34	1.30	0.608	0.368	1.433	0.708	0.497
0.250	1,324	0.912	0.906	0.383	0.220	0.709	0.271	0.308
0.167	0.238	0.090	0.439	0.033	0.008	0.008	0.005	0.100
0.083	0.139	0.057	0.319	0.022	0.004	0.003	0.001	0.020
0.000	0.022	0.031	0.216	0.005	0.000	0.001	0.001	0.093
N=0.1								
1.000	0.000	3.672	4.18	0.006	0.000	8.300	8.504	1.902
0.500	1.273	1.795	2.053	0.733	0.414	2.423	1.624	0.781
0.411	1.352	1.436	1.642	0.597	0.347	1.626	0.949	0.591
0.294	0.463	0.164	0.792	0.052	0.018	0.031	0.026	0.202
0.272	0.409	0.139	0.759	0.046	0.015	0.022	0.018	0.176
0.083	0.110	0.045	0.319	0.015	0.003	0.002	0.001	0.035
0.000	0.028	0.027	0.221	0.004	0.000	0.001	0.001	0.084
N=0.5								
1.000	0.000	2.247	4.18	0.003	0.000	3.387	3.454	1.146
0.748	0.566	1.621	3.097	0.377	0.142	1.949	1.704	0.805
0.667	0.710	1.414	2.735	0.360	0.152	1.538	1.264	0.695
0.581	0.837	1.174	2.325	0.314	0.144	1.115	0.848	0.575
0.500	0.916	0.896	1.851	0.231	0.111	0.698	0.490	0.453
0.457	0.920	0.723	1.645	0.168	0.081	0.486	0.338	0.394
N=1.5								
1.000	0.000	0.628	4.183	0.000	0.000	0.346	0.357	0.376
0.917	0.078	0.544	3.830	0.029	0.004	0.271	0.272	0.335
0.833	0.145	0.455	3.445	0.031	0.006	0.200	0.196	0.293
0.750	0.195	0.361	3.017	0.026	0.006	0.134	0.129	0.249
0.667	0.218	0.211	2.224	0.012	0.003	0.054	0.052	0.179
*0.625	0.216	0.201	2.179	0.011	0.003	0.050	0.049	0.174

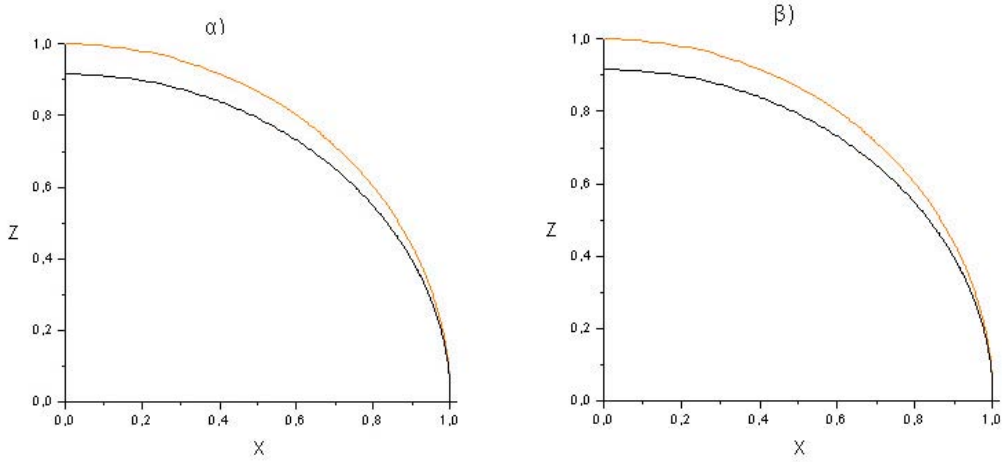


Figure 8: Meridional profile of rotating neutron stars with polytropic index and axis ratio $r_B = 0.917$ (a) $N=3.0$, (b) $N=4.0$

This sequence had been already obtained by Eriguchi and Sugimoto (1981) with the *SFNR* method. Their results are plotted in figures 9 and 10. In order to compare the present results with theirs, the models obtained by the *HSCF* method are indicated by crosses on these figures. In these figures another dimensional form of the angular momentum and angular velocity is used: $\Omega_0^2/4\pi G\bar{\rho}$ and $J^2/4\pi GM^{10/3}\bar{\rho}^{-1/3}$, where $\bar{\rho}$ the mean density defined by

$$\bar{\rho} = \frac{M}{V} \quad (195)$$

Of course, the results obtained with the *HSCF* method are in excellent agreement with those of Eriguchi and Sugimoto. As the axis ratio decreases, the equilibrium obtained numerically at each step moves along the Maclaurin sequence. When the newly defined squared angular velocity reaches 0.08726 (and at the same time the new squared angular momentum reaches 0.02174), then a bifurcation occurs and the configuration changes to what is called concave hamburger or pear-shaped. The bifurcation point is denoted by a filled circle in figures 3 and 4. The open circle stands for the point at which the axis ratio is zero. This is where the toroid sequence begins, which is also known as the Dyson-Wong sequence (Dyson 1893a,b; Wong 1974).

4.2 Differentially Rotating Polytropes

Two sequences of the polytropic index have been computed for the v -constant rotation law: $N=0$ and 1.5. Here the parameter d^2 in equation 111 is fixed at $0.01R_e^2$, i.e. $\hat{d}^2 = 0.01$. As d^2 becomes large, the rotation law approaches rigid rotation. On the other hand, the rotation law approaches true v -constant rotation when \hat{d}^2 vanishes. The results obtained for this case are summarized in Table II. The density distributions are shown in figure 11.

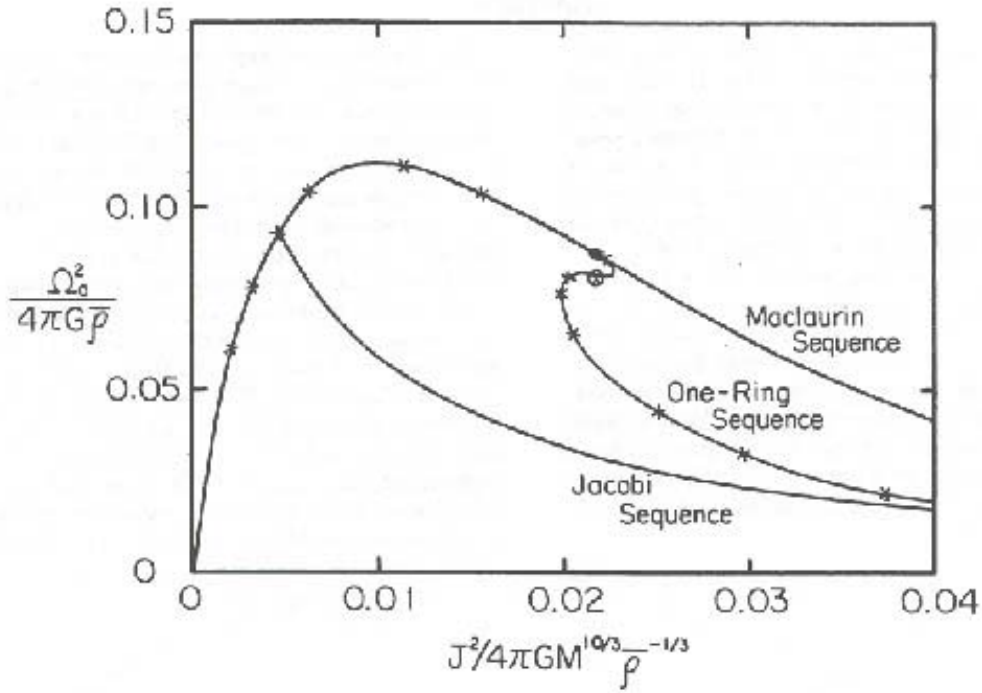


Figure 9: Dimensionless squared angular velocity $\Omega_0^2/4\pi G\bar{\rho}$ vs. dimensionless angular momentum $J^2/4\pi GM^{10/3}\bar{\rho}^{-1/3}$ for the Maclaurin, one-ring and the Jacobi sequences for which the polytropic index is $N=0.0$.

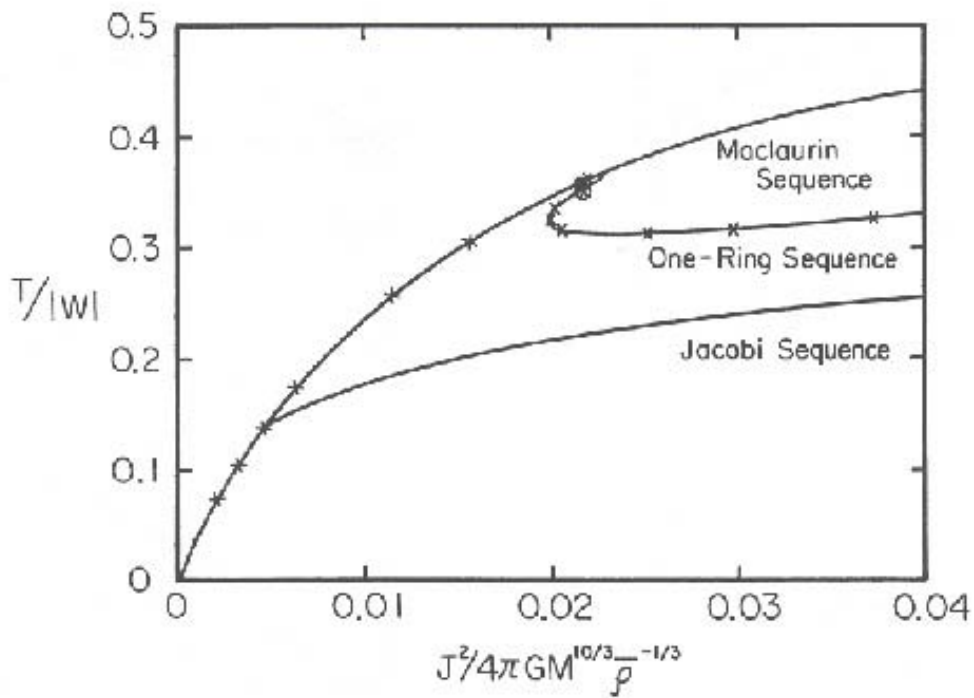


Figure 10: The rough stability factor $\tau = T/|W|$ vs. dimensionless squared angular momentum $J^2/4\pi GM^{10/3}\bar{\rho}^{-1/3}$ for the Maclaurin, one-ring and the Jacobi sequences for which the polytropic index is $N=0.0$.

TABLE II
Differential Rotation

r_B	$u_{\{0\}}^2$	M	V	J	T	-W	3Pi	Pmax
N=0.0								
0.750	0.194	3.721	3.681	1.011	0.350	8.017	7.463	1.431
0.667	0.369	3.173	3.270	1.124	0.540	7.134	6.112	1.189
0.333	0.460	2.375	2.302	1.163	0.668	4.433	3.708	0.897
0.250	1,324	0.912	0.906	0.383	0.220	0.709	0.271	0.308
0.167	0.354	0.111	0.569	4.76E-2	1.66E-2	1.25E-2	8.59E-3	1.43E-1
N=1.5								
0.750	0.068	0.681	3.681	0.071	0.019	0.428	0.369	0.331
0.667	0.089	0.673	3.302	0.084	0.029	0.404	0.342	0.309
0.333	0.246	0.615	2.602	0.153	0.056	0.353	0.218	0.257
0.250	0.063	0.033	1.668	1.62E-3	7.86E-4	2.16E-3	2.71E-3	9.55E-2
0.167	0.000	0.000	1.480	*****	*****	6.74E-7	1.62E-6	5.58E-2

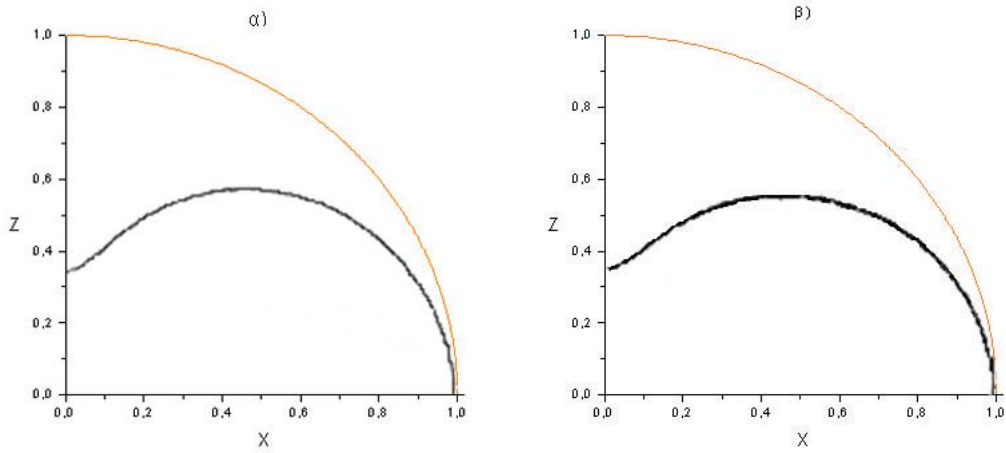


Figure 11: Meridional profile of differentially rotating polytropes having axis ratio $r_B = 0.333$ (a) $N=0.0$, (b) $N=1.5$

4.3 Extensions of the HSCF Method

We can apply the HSCF method to the case of zero-temperature white dwarfs, as it is mentioned in chapter 3. Another direct application of this method is the simulation of the Dyson-Wong sequence (i.e. toroidal configurations).

Moreover, we can extend this method to be applicable to a much wider range of objects without any difficulty. A first extension includes a three-dimensional SCF method, which enables us to compute a fission sequence from a dumbbell to a binary and also other multibody systems.

A second extension aims at computing a self-gravitating, rotating, accretion disk. Finally, a third extension concerns an axisymmetric and general relativistic case (Komatsu, Eriguchi and Hachisu 1986).

A APPENDIX

A.1 A Few Words on Legendre Polynomials

The Legendre function are the solution to the generalized Legendre equation

$$\frac{d}{dx} \left[(1-x^2) \frac{dP}{dx} \right] + \left[l(l+1) - \frac{m^2}{1-x^2} \right] P = 0 \quad (196)$$

where the function $P(\theta)$ is usually expressed in terms of $x = \cos \theta$ instead of θ itself. We will deal with a special case of this equation, in which $m^2 = 0$ thus yielding the ordinary Legendre differential equation

$$\frac{d}{dx} \left[(1-x^2) \frac{dP}{dx} \right] + l(l+1)P = 0 \quad (197)$$

We assume that the whole range of $\cos \theta$, including the north and south poles, is the region of interest. The desired solution should then be single valued, finite, and continuous on the interval $-1 \leq x \leq 1$ in order that it represent a physical potential. The solution will be assumed to be represented by a power series of the form

$$P(x) = x^\alpha \sum_{j=0}^{\infty} \alpha_j x^j \quad (198)$$

where α is a parameter to be determined. When this is substituted into 197, there results the series

$$\sum_{j=0}^{\infty} \{ (\alpha+j)(\alpha+j-1)\alpha_j x^{\alpha+j-2} - [(\alpha+j)(\alpha+j+1) - l(l+1)]\alpha_j x^{\alpha+j} \} = 0 \quad (199)$$

In this expansion the coefficient of each power of x must vanish separately. For $j = 0, 1$ we find that

$$\left. \begin{array}{l} \text{if } \alpha_0 \neq 0, \text{ then } \alpha(\alpha-1) = 0 \\ \text{if } \alpha_1 \neq 0, \text{ then } \alpha(\alpha+1) = 0 \end{array} \right\} \quad (200)$$

while for a general j value

$$\alpha_{j+2} = \left[\frac{(\alpha+j)(\alpha+j+1) - l(l+1)}{(\alpha+j+1)(\alpha+j+2)} \right] \alpha_j \quad (201)$$

A moment's thought shows that the two relations 200 are equivalent and that it is sufficient to choose either α_0 or α_1 different from zero, but not both. Making the former choice, we have $\alpha = 0$ or $\alpha = 1$. From 201 we see that the power series has only even powers of x ($\alpha = 0$) or only odd powers of x ($\alpha = 1$).

For either of the series α_0 or α_1 it is possible to prove the following properties:

- the series converges for $x^2 < 1$, regardless of the value of l
- the series diverges for $x = \pm 1$, unless it terminates.

Since we want a solution that is finite at $x = \pm 1$, as well as for $x^2 < 1$, we demand that the series terminate. Since α and j are positive integers or zero, the recurrence relation 201 will terminate only if l is zero or a positive integer. Even then only one of the two series converges at $x = \pm 1$. If l is even (odd), then only the $\alpha = 0$ ($\alpha = 1$) series terminates.¹¹ The polynomials in each case have x^l as their highest power of x , the next highest being x^{l-2} and so on, down to x^0 (x) for l even (odd). By convention, these polynomials are normalized to have the value unity at $x = +1$ and are called *Legendre polynomials* of order l , $P_l(x)$. The first few Legendre polynomials are:

$$\left. \begin{aligned} P_0(x) &= 1 \\ P_1(x) &= x \\ P_2(x) &= \frac{1}{2}(3x^2 - 1) \\ P_3(x) &= \frac{1}{2}(5x^3 - 3x) \\ P_4(x) &= \frac{1}{8}(35x^4 - 30x^2 + 3) \end{aligned} \right\} \quad (202)$$

By manipulation of the power series 198 and 201 it is possible to obtain a compact representation of the Legendre polynomials, known as the *Rodrigues Formula*

$$P_l(x) = \frac{1}{2^l l!} \frac{d^l}{dx^l} (x^2 - 1)^l \quad (203)$$

[cf. Arfken or Lebedev Special Functions and their Applications.]

The Legendre polynomials form a complete orthogonal set of functions on the interval $-1 \leq x \leq 1$. To prove the orthogonality we can appeal directly to Legendre's differential equation (DE). We write down the DE for $P_l(x)$, multiply by $P_{l'}(x)$ and then integrate over the interval:

$$\int_{-1}^1 P_{l'}(x) \left\{ \left[(1-x^2) \frac{dP_l}{dx} \right] + l(l+1)P_l(x) \right\} dx = 0 \quad (204)$$

Integrating the first term by parts we obtain

$$\int_{-1}^1 \left[(x^2 - 1) \frac{dP_l}{dx} \frac{dP_{l'}}{dx} + l(l+1)P_{l'}(x)P_l(x) \right] dx = 0 \quad (205)$$

If we now write down the latter equation with l and l' interchanged and subtract it from 205 the result is the orthogonality condition:

$$[(l(l+1) - l'(l'+1))] \int_{-1}^1 P_{l'}(x)P_l(x)dx = 0 \quad (206)$$

For $l \neq l'$, the integral must vanish. For $l = l'$, the integral assumes a finite value. To determine its value it is necessary to use an explicit representation of the Legendre polynomials, e.g. Rodrigues formula. Then the integral is explicitly:

$$N_l \equiv \int_{-1}^1 [P_l(x)]^2 dx = \frac{1}{2^{2l} (l!)^2} \int_{-1}^1 \frac{d^l}{dx^l} (x^2 - 1)^l \frac{d^l}{dx^l} (x^2 - 1)^l dx \quad (207)$$

¹¹For example, if $l = 0$ the $\alpha = 1$ series has a general coefficient $\alpha_j = \alpha_0/(j+1)$ for $j = 0, 2, 4, \dots$. Thus, the series is $\alpha_0(x + \frac{1}{3}x^3 + \frac{1}{5}x^5 + \dots)$. This is just α_0 times the power series expansion of a function $Q_0(x) = \frac{1}{2} \ln(1+x)/(1-x)$, which clearly diverges at $x = \pm 1$. For each l value there is a similar function $Q_l(x)$, with logarithms in it as the partner to the well behaved polynomial solution. See. Magnus et al. (pp.151 ff). Whittaker and Watson (Chapter XV) give a treatment using analytic functions.

Integration by parts l times yields the result

$$N_l = \frac{(-1)^l}{2^{2l}(l!)^2} \int_{-1}^1 (x^2 - 1)^l \frac{d^{2l}}{dx^{2l}} (x^2 - 1)^l dx \quad (208)$$

The differentiation $2l$ times of $(x^2 - 1)^l$ yields the constant $(2l)!$, so that

$$N_l = \frac{(2l)!}{2^{2l}(l!)^2} \int_{-1}^1 (1 - x^2)^l dx \quad (209)$$

The remaining integral can be done by brute force, by also by induction. We write the integrand as

$$(1 - x^2)^l = (1 - x^2)(1 - x^2)^{l-1} = (1 - x^2)^{l-1} + \frac{x}{2l} \frac{d}{dx} (1 - x^2)^l \quad (210)$$

Thus we have

$$N_l = \left(\frac{2l-1}{2l} \right) N_{l-1} + \frac{(2l-1)!}{2^{2l}(l!)^2} \int_{-1}^1 x d[(1 - x^2)^l] \quad (211)$$

Integration by parts in the last integral yields

$$N_l = \left(\frac{2l-1}{2l} \right) N_{l-1} - \frac{1}{2l} N_l \quad (212)$$

or

$$(2l+1)N_l = (2l-1)N_{l-1} \quad (213)$$

This shows that $(2l+1)N_l$ is independent of l . For $l=0$, where $P_0(x) = 1$, we have

$$(2l+1)N_l = N_0 = \int_{-1}^1 [1]^2 dx = 2 \quad (214)$$

and the orthogonality relation can be written

$$\int_{-1}^1 P_{l'}(x)P_l(x)dx = \frac{2}{2l+1} \delta_{l'l} \quad (215)$$

and the orthonormal functions are

$$U_l(x) = \sqrt{\frac{2l+1}{2}} P_l(x) \quad (216)$$

Since the Legendre polynomials form a complete set of orthogonal functions, any function $f(x)$ on the interval $-1 \leq x \leq 1$ can be expanded in terms of them. The Legendre series representation is

$$f(x) = \sum_{l=0}^{\infty} A_l P_l(x) \quad (217)$$

where

$$A_l = \frac{2l+1}{2} \int_{-1}^1 f(x)P_l(x)dx \quad (218)$$

As an example, consider the step function

$$f(x) = \begin{cases} +1, & \text{for } x > 0 \\ -1, & \text{for } x < 0 \end{cases} \quad (219)$$

Then

$$A_l = \frac{2l+1}{2} \left[\int_0^1 P_l(x) dx - \int_{-1}^0 P_l(x) dx \right] \quad (220)$$

Since $P_l(x)$ is odd (even) about $x = 0$ if l is odd (even), only the odd l coefficients are different from zero. Thus, for l odd,

$$A_l = (2l+1) \int_0^1 P_l(x) dx \quad (221)$$

By means of Rodrigues formula the integral can be evaluated, yielding

$$A_l = \left(-\frac{1}{2}\right)^{(l-1)/2} \frac{(2l+1)(l-2)!!}{2 \left(\frac{l+1}{2}\right)!} \quad (222)$$

where $(2n+1)!! = (2n+1)(2n-1)(2n-3)\cdots \times 5 \times 3 \times 1$. Thus, the series for $f(x)$ is

$$f(x) = \frac{3}{2}P_1(x) - \frac{7}{8}P_3(x) + \frac{11}{16}P_5(x) - \cdots \quad (223)$$

Certain recurrence relations among Legendre polynomials of different order are useful in evaluating integrals. From Rodrigues formula it is a straightforward matter to show that

$$\frac{dP_{l+1}}{dx} - \frac{dP_{l-1}}{dx} - (2l+1)P_l = 0 \quad (224)$$

This result combined with the DE 197 can be made to yield various recurrence formulas, some of which are:¹²:

$$(l+1)P_{l+1} - (2l+1)xP_l + lP_{l-1} = 0 \quad (225)$$

$$\frac{dP_{l+1}}{dx} - x \frac{dP_l}{dx} - (l+1)P_l = 0 \quad (226)$$

$$(x^2-1) \frac{dP_l}{dx} - lxP_l + lP_{l-1} = 0 \quad (227)$$

As an illustration of the use of these recurrence formulas, consider the evaluation of the integral

$$I = \int_{-1}^1 x P_l(x) P_l'(x) dx \quad (228)$$

By virtue of 225 we obtain an expression for $xP_l(x)$. Therefore I becomes

$$I = \frac{1}{2l+1} \int_{-1}^1 P_l'(x) [(l+1)P_{l+1}(x) + lP_{l-1}(x)] dx \quad (229)$$

¹²Recurrence formula 225 has been used calculate the Legendre polynomials needed to compute the gravitational potential, in our program for simulating rapidly rotating neutron stars.

The orthogonality integral can now be employed to show that the integral vanishes unless $l' = l \pm 1$, and that, for those values,

$$\int_{-1}^1 x P_l(x) P_{l'}(x) dx = \begin{cases} \frac{2(l+1)}{(2l+1)(2l+3)}, & \text{for } l' = l + 1 \\ \frac{2l}{(2l-1)(2l+1)}, & \text{for } l' = l - 1 \end{cases} \quad (230)$$

In a similar manner it is easy for one to show that

$$\int_{-1}^1 x^2 P_l(x) P_{l'}(x) dx = \begin{cases} \frac{2(l+1)(l+2)}{(2l+1)(2l+3)(2l+5)}, & \text{for } l' = l + 2 \\ \frac{2(2l^2+2l-1)}{(2l-1)(2l+1)(2l+3)}, & \text{for } l' = l \end{cases} \quad (231)$$

where it is assumed that $l' \geq l$.

B APPENDIX

B.1 Stationary Newtonian Star

In the present appendix we mention the model of a spherically symmetric polytropic star in hydrostatic equilibrium. The set of equations governing the equilibrium is

$$\frac{dP}{dr} = -\frac{Gm\rho}{r^2}, \quad (232)$$

and

$$\frac{dm}{dr} = -4\pi r^2 \rho \quad (233)$$

where r is the radial coordinate (we employ spherical coordinates), m is the mass contained in the interior of a sphere of radius r , G denotes the gravitational constant and P designates the pressure function. If we solve the set of equations, above, we obtain the pressure, the density distribution and the star's mass as functions of the radial coordinate, i.e., $P(r)$, $\rho(r)$ and $m(r)$. This set of functions describes the star uniquely (given a set of suitable boundary conditions). Other physical variables such as the radius R , the total mass M and the gravitational potential Φ , can be derived from the following equations

$$R = r|_{\rho=0} \quad (234)$$

$$M = M = mR \quad (235)$$

$$\nabla^2 \Phi = 4\pi G\rho. \quad (236)$$

It is noted that the set of differential equations 232 and 233 can be written into a compact form of a second order ordinary differential equation

$$\frac{d}{dr} \left(\frac{r^2}{\rho} \frac{dP}{dr} \right) = -4\pi G r^2 \rho \quad (237)$$

If we employ the dimensionless variables ξ and θ defined by

$$\begin{aligned} r &= \alpha\xi, \\ \rho &= \rho_c \theta^{\frac{1}{\gamma-1}}, \end{aligned} \quad (238)$$

where α is a proportionality parameter and ρ_c is the central density of the star (which, in this case happens to be the maximum density), the former equation can be reduced to a known second order, differential equation, if we choose the constant α to be

$$\alpha = \sqrt{\frac{K\gamma\rho_c^{\gamma-2}}{4\pi G(\gamma-1)}}, \quad (239)$$

Then we obtain the following equation, which is known as the *Lane-Emden* equation.

$$\frac{1}{\xi^2} \frac{d}{d\xi} \left(\xi^2 \frac{d\theta}{d\xi} \right) + \theta^{\frac{1}{\gamma-1}} = 0 \quad (240)$$

The solutions of Lane-Emden equation can be found numerically, for each γ value. However, they are available in the form of tables in international literature. There are some γ values such

as $\gamma = 6/5$, $\gamma = 2$ and $\gamma = \infty$ (the latter corresponds to the model of constant density) for which the solution $\theta(\xi)$ is analytic. For example when $\gamma = 2$ the solution is $\theta(\xi) = \sin \xi/\xi$.

If ξ_1 is the value of ξ on the surface of the star (at which the solution $\theta(\xi)$ vanishes for the first time), then the radius and the total mass of the star are respectively given by

$$R = \sqrt{\frac{K\gamma\rho_c^{\gamma-2}}{4\pi G(\gamma-1)}}\xi_1 \quad (241)$$

$$M = 4\pi \left[\frac{K\gamma\rho_c^{\gamma-2}}{4\pi G(\gamma-1)} \right]^{3/2} \rho_c \left| \frac{d\theta(\xi_1)}{d\xi} \right|, \quad (242)$$

where we have taken into account that $\theta(\xi)$ assumes its maximum value and its first derivative with respect to ξ vanishes $d\theta/d\xi = 0$ on the star's surface. This condition is imposed by the symmetry of the problem and the assumption of equilibrium.

Next, we present a way to solve numerically the Lane-Emden equation

B.2 Numerical Solution

In order to solve the Lane-Emden equation first we have to reduce it to a set of two ordinary, first order differential equations. It is noted that this is not the only path one may follow. For example, we could solve the original set of equations, after defining a set of dimensionless variables. In the present work we will solve the Lane-Emden equation through a fourth-order Runge-Kutta numerical scheme.

We define a new variable $q = d\theta/d\xi$ so that equation 240 become equivalent to the following set of equations

$$\begin{aligned} \frac{d\theta}{d\xi} &= q \\ \frac{dq}{d\xi} &= -\frac{2}{\xi}q - \theta^{\frac{1}{\gamma-1}}. \end{aligned} \quad (243)$$

As already mentioned, we will solve this system by virtue of the Runge-Kutta method. We now, formulate the general form of this method

For a set of equations of the form

$$\begin{aligned} \frac{dy}{dx} &= f(x, y, z) \\ \frac{dz}{dx} &= g(x, y, z) \end{aligned} \quad (244)$$

we use a sequence of discretized points (one-dimensional mesh) x_0, x_1, \dots, x_n , where $n+1$ is the total mesh number. These points are equally spaced by $h = x_n - x_{n-1}$. By providing the initial values y_0 and z_0 at point x_0 , the solution at the next iteration step can be found by virtue of the following recurrence formulas

$$\begin{aligned} y_{n+1} &= y_n + \frac{1}{6}(k_1 + 2k_2 + 2k_3 + k_4) \\ z_{n+1} &= z_n + \frac{1}{6}(l_1 + 2l_2 + 2l_3 + l_4), \end{aligned} \quad (245)$$

where

$$\begin{aligned}
k_1 &= hf(x_n, y_n, z_n) \\
l_1 &= hg(x_n, y_n, z_n) \\
k_2 &= hf(x_n + \frac{1}{2}h, y_n + \frac{1}{2}k_1, z_n + \frac{1}{2}l_1) \\
l_2 &= hg(x_n + \frac{1}{2}h, y_n + \frac{1}{2}k_1, z_n + \frac{1}{2}l_1) \\
k_3 &= hf(x_n + \frac{1}{2}h, y_n + \frac{1}{2}k_2, z_n + \frac{1}{2}l_2) \\
l_3 &= hg(x_n + \frac{1}{2}h, y_n + \frac{1}{2}k_2, z_n + \frac{1}{2}l_2) \\
k_4 &= hf(x_n + h, y_n + k_3, z_n + l_3) \\
l_4 &= hg(x_n + h, y_n + k_3, z_n + l_3)
\end{aligned} \tag{246}$$

For the equation under consideration 243, the initial conditions at the center ($x_0 = 0$) of the star are

$$\rho = \rho_c \tag{247}$$

$$\frac{d\rho}{dr} = 0 \tag{248}$$

i.e.

$$\theta = 1 \tag{249}$$

$$\frac{d\theta}{d\xi} = 0 \tag{250}$$

which yields

$$y(x_0) = y_0 = 1 \tag{251}$$

$$z(x_0) = z_0 = 0 \tag{252}$$

However, the second equation of 243 has a pole at $\xi = 0$. A treatment for this problem can be provided by expanding the function $\theta(\xi)$ in ordinary Taylor series. We then obtain

$$\theta(\xi) = \theta(0) + \xi\theta'(0) + \frac{1}{2}\xi^2\theta''(0) \tag{253}$$

Thus,

$$\theta(\xi) = 1 + \frac{1}{2}\xi^2\theta''(0) \tag{254}$$

if we differentiate the former equation, we find

$$\theta'(\xi) = q = \xi\theta''(0) \tag{255}$$

Then, system 243 can be written as follows

$$\frac{d\theta}{d\xi} = \xi\theta''(0) \quad (256)$$

and

$$\frac{dq}{d\xi} = -2\theta''(0) - \left[1 + \frac{1}{2}\xi^2\theta''(0)\right]^{\frac{1}{\gamma-1}} \quad (257)$$

Hence, we need $\theta''(0)$ for our calculations. $\theta''(0)$ must be negative, for $\theta(\xi)$ must assume maximum value at the center of the star. Of course, all these hold true only if $\xi \ll 1$, a requirement which actually holds true, since we are going to use this trick only at the first step of the iteration scheme, i.e. when $\xi = 10^{-4}$ or 10^{-6} . When $\xi = 0$, equation 257 yields $\theta''(0) = -\frac{1}{3}$. We eventually obtain,

$$\frac{dq}{d\xi} = \frac{2}{3} - \left[1 - \frac{1}{6}\xi^2\right]^{\frac{1}{\gamma-1}} \quad (258)$$

and

$$\frac{d\theta}{d\xi} = -\frac{1}{3}\xi \quad (259)$$

Special case N=0. In the case for which the polytropic index is 0, the polytropic exponent which is defined by

$$\gamma = 1 + \frac{1}{N} \quad (260)$$

becomes infinite. Then, it is quite straightforward that the function $\theta(\xi) = 1$ is the solution to the Lane-Emden equation.

C APPENDIX

C.1 Program for the HSCF Method

In the resent appendix, we present the program, written in FORTRAN 90/95, which implements the HSCF method.

```
!      Last change: AS   25 Jun 2003   7:23 pm
!*****
!*      Program for Izumi Hachisu's Self-Consistent Field Method      *
!*****

!-----
! Explanation of notation used in the program
!-----

! P      == Legendre Polynomial
! gamma  == Polytropic power  $P=K*\rho^{\{\gamma\}}$ 
! Nu     == Polytropic Index
! sumM   == Variable used to compute the sum in the calculation of
! the star's Mass
! sumW   == Variable used to compute the sum in the calculation of
! the star's Gravitational Energy
! sumPi1 == Variable used to compute the sum in the calculation of
! the star's Pressure's volume integral
! sumJ1  == Variable used to compute the sum in the calculation of
! the star's angular momentum
! sumT   == Variable used to compute the sum in the calculation of
! the star's Rotational Energy
! sumV   == Variable used to compute the sum in the calculation of
! the star's Volume
! d      == Deviation from true u-constant differential rotation parameter
! delta  == Accuracy parameter
! Prmax  == Star's maximum Pressure
! Mass   == Star's mass
! W      == Star's gravitational energy
! Pi1    == Star's pressure's volume integral
! T      == Star's rotational energy
! J1     == Star's angular momentum
! V      == Star's volume
! rs     == Surface's points distanse from the origin
! test1, test2, test3 == Accuracy condition parameters
! pi     == 3,14159
! Rmax   == Star's maximum radius
! rB     == Point B's distanse from the origin
! Hmax   == Maximum enthalpy
! h02    ==  $h_{\{0\}}^{\{2\}}$ 
! C      == Constant incorporated with the calculation of enthalpy
! Hmaxold == Old value of Hmax
! h02    == Old value of h02
```

```

! Cold    == Old value of C
! hr      == mesh step in the r-direction
! hmu     == mesh step in the \mu-direction
! X       == \ksi (Lane Emden equation)
! Y       == \theta(\ksi) (Lane Emden equation)
! Z       == d\theta/d\ksi (Lane Emden equation)
! r       == Mesh points in the r-direction matrix
! mu      == Mesh points in the \mu-direction matrix
! Rbound  == Surface's points distance matrix
! rB      == Point B's distance matrix
! P2N     == Legendre Polynomials Matrix
! rho     == Density distribution matrix
! Phi     == Gravitational Potential matrix
! H       == Enthalpy matrix
! Pr      == Pressure matrix
! F2N     == Green's function matrix

```

```

!-----
!-----

```

```
PROGRAM HSCF
```

```
IMPLICIT NONE
```

```

REAL(8) :: P
REAL(8) :: gamma,Nu,upper
REAL(8) :: sumM,sumW,sumPi1,sumJ1,sumT,sumV
REAL(8) :: d=0.1,delta,Prmax,Mass,W,Pi1,T,J1,V,rs,test1,test2,test3,test
REAL(8) :: pi,Rmax,Hmax,h02,C,Hmaxold,h02old,Cold,hr,hmu
REAL(8), ALLOCATABLE, DIMENSION(:) :: X,Y,Z
REAL(8), ALLOCATABLE, DIMENSION(:) :: r,mu,Rbound,rB
INTEGER, ALLOCATABLE, DIMENSION(:) :: JrB
REAL(8), ALLOCATABLE, DIMENSION(:,) :: P2N,rho,Phi,H,Pr
REAL(8), ALLOCATABLE, DIMENSION(:,,:,:) :: F2N
INTEGER :: n,KDIV,NDIV,STATUS,i,j,Lmax,l,k,m,jB,nB,m1

```

```

!=====
!=====

```

```

PRINT*,'Give the accuracy parameter delta: '
READ*,delta
PRINT*,'Give the polytropic index Nu: '
READ*,Nu
PRINT*,'Give mesh number "KDIV" in mu direction: '
READ*,KDIV

```

```

PRINT*, 'Give mesh number "NDIV" in r direction: '
READ*, NDIV
PRINT*, 'Give maximum number Lmax of legendre polynomials: '
READ*, Lmax

ALLOCATE(r(NDIV), mu(KDIV), P2N(KDIV, 0:Lmax), rB(13), JrB(13), &
          F2N(NDIV, NDIV, 0:Lmax), rho(KDIV, NDIV), Pr(KDIV, NDIV), &
          Phi(KDIV, NDIV), H(KDIV, NDIV), Rbound(KDIV), STAT=STATUS)
IF (STATUS/=0) STOP 'Not enough memory'

r=0d0; mu=0d0; rB=0d0; JrB=0; P2N=0d0; F2N=0d0; rho=0d0; Pr=0d0; &
Phi=0; H=0; Rbound=0

pi=4d0*ATAN(1d0)
Rmax=16d0/15d0
hr=Rmax/(NDIV-1d0)
hmu=1d0/(KDIV-1d0)

!Calculation of the test density distribution

IF (Nu==0.) THEN
rho=1d0
ELSE
PRINT*, 'Calculation of the test density'
gamma=1d0+1d0/Nu
ALLOCATE(X(NDIV), Y(NDIV), Z(NDIV), STAT=STATUS)
IF (STATUS/=0) STOP 'Not enough memory'

PRINT*, 'Give upper and lower bounds: '
READ*, upper, X(1)
Y(1)=1d0; Z(1)=0d0

CALL RK4(X, Y, Z, upper)
DO m1=1, KDIV
rho(:, m1)=Y(m1)
END DO

END IF

!=====
!=====

!=====
!=====

```

```
!Mesh points in the r-direction
```

```
DO j=1,NDIV  
r(j)=Rmax*(j-1d0)/(NDIV-1d0)  
END DO
```

```
!Mesh points in the mu-direction
```

```
DO i=1,KDIV  
mu(i)=(i-1d0)/(KDIV-1d0)  
END DO  
OPEN(2,FILE='mu_mesh.dat')  
DO i=1,KDIV  
WRITE (2,200) mu(i)  
END DO  
CLOSE(2)
```

```
! Mesh points in the r-direction for point B
```

```
rB=(/r(15*(NDIV-1)/16+1),r(91),r(61),r(46),r(31),r(16),r(1),-r(16)&  
-r(31),-r(46),-r(61),-r(91),-r(15*(NDIV-1)/16+1)/)  
JrB=(/15*(NDIV-1)/16+1,91,61,46,31,16,1,16,31,46,61,91,15*(NDIV-1)/16+1/)
```

```
!=====  
!=====
```

```
!=====  
!=====
```

```
!Calculation of Legendre Polynomials
```

```
DO n=0,Lmax  
DO l=1,KDIV  
CALL LGND(2*n,mu(1),P)  
P2N(l,n)=P  
END DO  
END DO
```

```
!=====  
!=====
```

```
!=====  
!=====
```

```
!Calculation of Green's Function f_{2n}
```

```

DO n=0,Lmax
  DO k=1,NDIV
    DO l=1,NDIV
      F2N(k,l,n)=G2N(2*n,r1=r(k),r2=r(l))
    END DO
  END DO
END DO

```

```

!=====
!=====

```

```

!=====
!=====

```

```

!=====
!=====
!*****
!=====
!=====

```

```

! Main iteration routine

```

```

OPEN (1,FILE='N00.dat')

```

```

Point B loop: DO jB=1,13

```

```

WRITE(1,*) '=====',
WRITE(1,*) ' r_B    h02    M    V    J    T    -W    3Pi    Pmax ',
WRITE(1,*) '-----',
WRITE(1,10) 'N=',Nu
WRITE(1,*) '-----',

```

```

PRINT*,rB(jB)

```

```

Hmaxold=0d0;h02old=0d0;Cold=0d0

```

```

Accuracy loop: DO

```

```

nB=1

```

```

! Calculation of the quantity designated by  $D^{\{1\}}_{\{k,n\}}$ 

```

```

DO k=1,KDIV
  DO n=0,Lmax
    sumD1=0d0
    DO i=1,KDIV-2,2

```

```

        sumD1=sumD1+(hmu/3d0)*(P2N(i,n)*&
            rho(i,k)+4d0*P2N(i+1,n)*rho(i+1,k)&
            +P2N(i+2,n)*rho(i+2,k))
    END DO
    D11(k,n)=sumD1
END DO
END DO

! Calculation of the quantity designated by  $D^{\{2\}}_{\{n,j\}}$ 

DO n=0,Lmax
    DO j=1,NDIV
        sumD2=0d0
        DO k=1,NDIV-2,2
            sumD2=sumD2+(hr/3d0)*(F2N(k,j,n)*D11(k,n)+&
                4d0*F2N(k+1,j,n)*D11(k+1,n)+&
                F2N(k+2,j,n)*D11(k+2,n))
        END DO
        D22(n,j)=sumD2
    END DO
END DO

! Calculation of the Gravitational Potential  $\Phi(\mu,r)$ 

DO i=1,KDIV
    DO j=1,NDIV
        sumPhi=0d0
        DO n=0,Lmax
            sumPhi = sumPhi+D22(n,j)*P2N(i,n)
        END DO
        Phi(i,j)=-4d0*pi*sumPhi
    END DO
END DO

! Calculation of the Enthalpy H

IF (jB.LE.7) THEN
    h02=-(Phi(1,15*(NDIV-1)/16+1)-Phi(KDIV,JrB(jB)))/&
        (PsiRGD(0d0,1d0)-PsiRGD(1d0,rB(jB)))
ELSE
    h02=-(Phi(1,15*(NDIV-1)/16+1)-Phi(1,JrB(jB)))/& ! For ring-like structures
        (PsiRGD(0d0,1d0)-PsiRGD(0d0,ABS(rB(jB))))
END IF

C=Phi(1,15*(NDIV-1)/16+1)+h02*PsiRGD(0d0,1d0)

```

```

DO  i=1,KDIV
    DO  j=1,NDIV
        H(i,j)=C-Phi(i,j)-h02*PsiRGD(mu(i),r(j))
    END DO
END DO

Hmax=MAXVAL(H)

! Improved Density Distribution

DO  i=1,KDIV
    DO  j=1,NDIV
        IF (H(i,j)>0d0) THEN
            rho(i,j)=(H(i,j)/MAXVAL(H))**Nu
        ELSE
            rho(i,j)=0d0
        END IF
    END DO
END DO

! Accuracy condition

test1=ABS((Hmax-Hmaxold)/Hmax)
test2=ABS((h02-h02old)/h02)
test3=ABS((C-Cold)/C)

IF (test1.LT.delta.AND.test2.LT.delta.AND.test3.LT.delta) EXIT

Hmaxold=Hmax
h02old=h02
Cold=C

nB=nB+1

END DO Accuracy loop

! Calculation of the star's Pressure

Pr=1d0/(Nu+1d0)*H*rho

Prmax=MAXVAL(Pr)

! Calculation of the Star's Mass

sumM=0d0

```

```

DO j=1,NDIV-2,2
sumM=sumM+(hr/3d0)*(r(j)**2*Q1(j)+&
          4d0*r(j+1)**2*Q1(j+1)+r(j+2)**2*Q1(j+2))
END DO
Mass=4d0*pi*sumM

! Calculation of the Star's gravitational potential energy

sumW=0d0
DO j=1,NDIV-2,2
sumW=sumW+(hr/3d0)*(r(j)**2*S1(j)+&
          4d0*r(j+1)**2*S1(j+1)+r(j+2)**2*S1(j+2))
END DO
W=2d0*pi*sumW

! Calculation of the Pressure's volume integral

sumPi1=0d0
DO j=1,NDIV-2,2
sumPi1=sumPi1+(hr/3d0)*(r(j)**2*G1(j)+&
          4d0*r(j+1)**2*G1(j+1)+r(j+2)**2*G1(j+2))
END DO
Pi1=4d0*pi*sumPi1

! Calculation of the star's angular momentum

sumJ1=0d0
DO j=1,NDIV-2,2
sumJ1=sumJ1+(hr/3d0)*(r(j)**4*Q2(j)+&
          4d0*r(j+1)**4*Q2(j+1)+r(j+2)**4*Q2(j+2))
END DO
J1=4d0*pi*sumJ1

! Calculation of the star's rotational energy

sumT=0d0
DO j=1,NDIV-2,2
sumT=sumT+(hr/3d0)*(r(j)**4*S2(j)+&
          4d0*r(j+1)**4*S2(j+1)+r(j+2)**4*S2(j+2))
END DO
T=2d0*pi*sumT

! Calculation of the star's boundary surface

DO i=1,KDIV

```

```

DO j=1,KDIV-1
  test=H(i,j+1)*H(i,j)
  IF (test.LT.0d0) CALL Lagrange(r(j),r(j+1),H(i,j),H(i,j+1),rs)
END DO
Rbound(i)=rs
END DO

! Calculation of the star's volume

sumV=0d0
DO i=1,KDIV-2,2
sumV=sumV+(hmu/3d0)*(Rbound(i)**3+4d0*Rbound(i+1)**3+Rbound(i+2)**3)
END DO
V=(4d0/3d0)*pi*sumV

WRITE(1,100) rB(jB),h02,Mass,V,J1,T,-W,3*Pi1,Prmax
WRITE(1,*) ' - -----'
WRITE(1,*) '      Rbound'
WRITE(1,*) ' -----'
WRITE(1,*) ' X '
DO i=1,KDIV
WRITE(1,200) Rbound(i)*(1-mu(i)**2)**(1d0/2d0)
END DO

WRITE(1,*) ' Z '
DO i=1,KDIV
WRITE(1,200) Rbound(i)*mu(i)
END DO

PRINT 100,rB(jB),h02,Mass,V,J1,T,-W,3*Pi1,Prmax

END DO Point B loop

CLOSE (1)

10 FORMAT (T31,A3,F3.1)
100 FORMAT (2x,F6.3,2x,F5.3,2x,F5.3,2x,F5.3,2x,F5.3,2x,F6.3,2x,F7.3,&
2x,F7.3,2x,F5.3)
200 FORMAT (T6,F5.3)

!=====
!=====
!*****
!=====
!=====

```

```
!*****
!*****
```

CONTAINS

```
!-----
! SUBROUTINES FOR COMPUTING THE TEST DENSITY DISTRIBUTION
! USING THE LANE-EMDEN EQUATION
```

! 4th order Runge-Kutta algorithm

```
      SUBROUTINE RK4(X,Y,Z,b)
      REAL(8)::X(:),Y(:),Z(:),b,h,k1,k2,k3,k4,l1,l2,l3,l4
      INTEGER(4)::i

      h=ABS(b-X(1))/SIZE(X)
      PRINT*, 'h=',h

      DO i=1,SIZE(X)-1

         k1=h*F(Z(i))

         IF (i.EQ.1) THEN
            l1=h*W1(X(i))
         ELSE
            l1=h*G(X(i),Y(i),Z(i))
         END IF

         k2=h*F(Z(i)+1d0/2d0*l1)
         l2=h*G(X(i)+1d0/2d0*h,Y(i)+1d0/2d0*k1,Z(i)+1d0/2d0*l1)
         k3=h*F(Z(i)+1d0/2d0*l2)
         l3=h*G(X(i)+1d0/2d0*h,Y(i)+1d0/2d0*k2,Z(i)+1d0/2d0*l2)
         k4=h*F(Z(i)+l3)
         l4=h*G(X(i)+h,Y(i)+k3,Z(i)+l3)

         Y(i+1)=Y(i)+1d0/6d0*(k1+2d0*k2+2d0*k3+k4)
         Z(i+1)=Z(i)+1d0/6d0*(l1+2d0*l2+2d0*l3+l4)
         X(i+1)=X(i)+h
      END DO
      END SUBROUTINE
```

```
! Lane-Emden Differential equation Function for dy/dx
```

```
REAL(8) FUNCTION F(q)
REAL(8),INTENT(IN) ::q
F=q
END FUNCTION F
```

```
! Lane-Emden Differential equation Function for  $d^2y/dx^2$ 
```

```
REAL(8) FUNCTION G(kxi,theta,q)
REAL(8),INTENT(IN) ::kxi,theta,q
G=-2d0/kxi*q-theta**(1d0/(gamma-1d0))
END FUNCTION G
```

```
! Lane-Emden Differential equation Function for  $d^2y/dx^2$ 
```

```
! used only in the first iteration
```

```
REAL(8) FUNCTION W1(kxi)
REAL(8),INTENT(IN) ::kxi
W1=2d0/3d0-(1d0-(1d0/6d0)*kxi**2)**(1d0/(gamma-1d0))
END FUNCTION W1
```

```
! End of subroutine for the test density
```

```
!-----
```

```
! Subroutine to generate Legendre Polynomials
```

```
! of degree n with argument xx
```

```
SUBROUTINE LGND(n,xx,p)
REAL(8), INTENT(IN) :: xx
INTEGER, INTENT(IN) :: n
REAL(8), INTENT(OUT)::p
INTEGER :: i
REAL(8) :: pleg(0:n)
```

```
pleg(0)=1d0
pleg(1)=xx
DO i=2,n
pleg(i) =((2*i-1)*xx*pleg(i-1)-(i-1)*pleg(i-2))/i
END DO
p=pleg(n)
```

```
END subroutine LGND
```

! Function for computing the Green's function $f_{\{2n\}}(r',r)=G2N$,
! associated with the calculation of the Gravitational Potential

```

REAL(8) FUNCTION G2N(n,r1,r2)
REAL(8), INTENT(IN) :: r1,r2
INTEGER, INTENT(IN) :: n

IF (r1<r2) THEN
G2N=r1**(n+2)/r2**(n+1)
ELSE if (r1>r2) THEN
G2N=r2**(n)/r1**(n-1)
ELSE
G2N=1d0
END IF
END FUNCTION G2N

```

! Subroutine used for computing $D1(k,n)$ in the gravitational potential

```

REAL(8) FUNCTION D1(k1,n1,dens) RESULT(sum1)
INTEGER, INTENT(IN) :: k1,n1
REAL(8), INTENT(IN) :: dens(:, :)
INTEGER :: i1
sum1=0d0

DO i1=1,KDIV-2,2
sum1=sum1+(hmu/3d0)*(P2N(i1,n1)*&
                dens(i1,k1)+4d0*P2N(i1+1,n1)*dens(i1+1,k1)&
                +P2N(i1+2,n1)*dens(i1+2,k1))
END DO

END FUNCTION D1

```

! Subroutine used for computing $D2(n,j)$ in the gravitational potential

```

REAL(8) FUNCTION D2(n1,j1,D11) RESULT(sumD2)
REAL(8), INTENT(IN) :: D11(:, :)
INTEGER, INTENT(IN) :: j1,n1
INTEGER :: k
sumD2=0d0

DO k=1,NDIV-2,2
sumD2=sumD2+(hr/3d0)*(F2N(k,j1,n1)*D11(k,n1)+&
                4d0*F2N(k+1,j1,n1)*D11(k+1,n1)+&
                F2N(k+2,j1,n1)*D11(k+2,n1))
END DO

END FUNCTION D2

```

! Subroutine for the calculation of the Gravitational Potential

```
SUBROUTINE GravPot(D22,Pot)
REAL(8), INTENT(IN) :: D22(:,,:)
REAL(8), INTENT(OUT) :: Pot(:,,:)
REAL(8) :: sumPot
INTEGER :: i,j,n

DO i=1,KDIV
  DO j=1,NDIV
    sumPot=0d0
    DO n=0,Lmax
      sumPot = sumPot+D22(n,j)*P2N(i,n)
    END DO
    Pot(i,j)=-4d0*pi*sumPot
  END DO
END DO

END SUBROUTINE GravPot
```

! Rotation Laws

! A) Rigid rotation

```
! (i) The psi function
REAL(8) FUNCTION PsiRGD(mu,r)
REAL(8), INTENT(IN) :: mu,r
PsiRGD=-(1d0/2d0)*r**2*(1-mu**2)
END FUNCTION PsiRGD
```

```
! (ii) The Omega function
REAL(8) FUNCTION OmegaRGD(mu,r)
REAL(8), INTENT(IN) :: mu,r
OmegaRGD=h02**(1d0/2d0)
END FUNCTION OmegaRGD
```

! B) Differential u-constant rotation

```
! (i) The psi function
REAL(8) FUNCTION PsiUCT(mu,r)
REAL(8), INTENT(IN) :: mu,r
PsiUCT=-(1d0/2d0)*LOG(1d0+r**2*(1-mu**2)/d**2)
```

```
END FUNCTION PsiUCT
```

```
!) (ii) The Omega Function  
REAL(8) FUNCTION OmegaUCT(mu,r)  
REAL(8), INTENT(IN) :: mu,r  
OmegaUCT=(ABS(h02/(d**2+r**2*(1-mu**2))))**(1d0/2d0)  
END FUNCTION OmegaUCT
```

```
! Subroutine used for computing Q1(j) incorporated  
! with the calculation of the star's Mass
```

```
REAL(8) FUNCTION Q1(j1) RESULT(sumQ1)  
INTEGER, INTENT(IN) :: j1  
INTEGER :: i1  
sumQ1=0d0  
  
DO i1=1,KDIV-2,2  
sumQ1=sumQ1+(hmu/3d0)*(rho(i1,j1)+&  
4d0*rho(i1+1,j1)+rho(i1+2,j1))  
END DO  
  
END FUNCTION Q1
```

```
! Subroutine used for computing S1(j) incorporated  
! with the calculation of the gravitational energy
```

```
REAL(8) FUNCTION S1(j2) RESULT(sumS1)  
INTEGER, INTENT(IN) :: j2  
INTEGER :: i2  
sumS1=0d0  
  
DO i2=1,KDIV-2,2  
sumS1=sumS1+(hmu/3d0)*(rho(i2,j2)*Phi(i2,j2)+&  
4d0*rho(i2+1,j2)*Phi(i2+1,j2)+rho(i2+2,j2)*Phi(i2+2,j2))  
END DO  
  
END FUNCTION S1
```

```
! Subroutine used for computing G1(j) incorporated  
! with the calculation of the volume integral of Pressure
```

```
REAL(8) FUNCTION G1(j3) RESULT(sumG1)  
INTEGER, INTENT(IN) :: j3  
INTEGER :: i3  
sumG1=0d0
```

```

DO i3=1,KDIV-2,2
sumG1=sumG1+(hmu/3d0)*(Pr(i3,j3)+&
                4d0*Pr(i3+1,j3)+Pr(i3+2,j3))
END DO

```

```

END FUNCTION G1

```

```

! Subroutine used for computing Q2(j) incorporated
! with the calculation of the angular momentum J.
! This subroutine is written so that it computes the rigid
! rotation case. To change to the differential rotation
! model just replace the function OmegaRGD by the function
! OmegaUCT

```

```

REAL(8) FUNCTION Q2(j4) RESULT(sumQ2)
INTEGER, INTENT(IN) :: j4
INTEGER :: i4
sumQ2=0d0

DO i4=1,KDIV-2,2
sumQ2=sumQ2+(hmu/3d0)*&
    (OmegaRGD(mu(i4),r(j4))*rho(i4,j4)*(1-mu(i4))**(1d0/2d0)+&
    4d0*OmegaRGD(mu(i4+1),r(j4))*rho(i4+1,j4)*(1-mu(i4+1))**(1d0/2d0)+&
    OmegaRGD(mu(i4+2),r(j4))*rho(i4+2,j4)*(1-mu(i4+2))**(1d0/2d0))
END DO

```

```

END FUNCTION Q2

```

```

! Subroutine used for computing S2(j) incorporated
! with the calculation of the star's rotational energy T.
! This subroutine is written so that it computes the rigid
! rotation case. To change to the differential rotation
! model just replace the function OmegaRGD by the function
! OmegaUCT

```

```

REAL(8) FUNCTION S2(j5) RESULT(sumS2)
INTEGER, INTENT(IN) :: j5
INTEGER :: i5
sumS2=0d0

DO i5=1,KDIV-2,2
sumS2=sumS2+(hmu/3d0)*&
    ((OmegaRGD(mu(i5),r(j5))**2*rho(i5,j5)*(1-mu(i5))**(1d0/2d0)+&
    4d0*(OmegaRGD(mu(i5+1),r(j5))**2*rho(i5+1,j5)*(1-mu(i5+1))**(1d0/2d0)+&
    (OmegaRGD(mu(i5+2),r(j5))**2*rho(i5+2,j5)*(1-mu(i5+2))**(1d0/2d0))
END DO

```

```

END FUNCTION S2

```

```
! Lagrange Linear Interpolation Subroutine
```

```
SUBROUTINE Lagrange(r1,r2,H1,H2,r)  
REAL(8), INTENT(IN) :: r1,r2,H1,H2  
REAL(8), INTENT(OUT) :: r
```

```
r=(r2*H1-r1*H2)/(H1-H2)
```

```
END SUBROUTINE Lagrange
```

```
END PROGRAM HSCF
```

List of Figures

1	The eccentricity e and the ellipticity f along the Maclaurin sequence, as a function of $\tau = K/ W $	21
2	The squared angular velocity Ω^2 and the total angular momentum J along the Maclaurin sequence, as a functions of $\tau = K/ W $. Ordinates on the left and on the right refer to Ω^2 and J , respectively	22
3	Two points on the boundary surface, determine uniquely a stellar model :(a) spheroidal structure, (b) toroidal structure.	32
4	Meridional profile of rotating neutron stars with polytropic index $N=0.0$: (a)axis ratio $r_B = 0.5$, (b) axis ratio $r_B = 0.333$	43
5	Meridional profile of rotating neutron stars with polytropic index $N=0.1$: (a)axis ratio $r_B = 0.5$, (b) axis ratio $r_B = 0.411$	43
6	Meridional profile of rotating neutron stars with polytropic index $N=0.5$: (a)axis ratio $r_B = 0.748$, (b) axis ratio $r_B = 0.581$	44
7	Meridional profile of rotating neutron stars with polytropic index $N=1.5$: (a)axis ratio $r_B = 0.75$, (b) axis ratio $r_B = 0.625$, this is a critical rotation case.	44
8	Meridional profile of rotating neutron stars with polytropic index and axis ratio $r_B = 0.917$ (a) $N=3.0$, (b) $N=4.0$	46
9	Dimensionless squared angular velocity $\Omega_0^2/4\pi G\bar{\rho}$ vs. dimensionless angular momentum $J^2/4\pi GM^{10/3}\bar{\rho}^{-1/3}$ for the Maclaurin, one-ring and the Jacobi sequences for which the polytropic index is $N=0.0$	47
10	The rough stability factor $\tau = T/ W $ vs. dimensionless squared angular momentum $J^2/4\pi GM^{10/3}\bar{\rho}^{-1/3}$ for the Maclaurin, one-ring and the Jacobi sequences for which the polytropic index is $N=0.0$	47
11	Meridional profile of differentially rotating polytropes having axis ratio $r_B = 0.333$ (a) $N=0.0$, (b) $N=1.5$	48

References

- [1] Jean Luis Tassoul. *Theory of Rotating Stars*.
Princeton Series in Astrophysics.
- [2] Kellogg, O.D. *Foundations of Potential Theory*
New York: Ungar Publishing Co., 1929 (New York: Dover Public., Inc., 1954).
- [3] W. F. Hughes & J.A. Brighton. *Theory and Problems of Fluid Dynamics*.
Schaum Publ. Co., 1967.
- [4] Izumi Hachisu. *A Versatile Method for Obtaining Structures of Rapidly Rotating Stars*.
The Astrophysical Journal Supplement Series, 61:479-507, 1986 July.
- [5] Y. Eriguchi, D. Sugimoto 1981. *Progr. Theoret. Phys.*, 65,1870.
- [6] John David Jackson. *Classical Electrodynamics Third Edition*.
John Willey & Sons, Inc. New York Chichester Weinheim.
- [7] P. M. Morse and H. Feshbach. *Methods of Theoretical Physics*.
International Series of Pure and Applied Physics.
- [8] N.N. Lebedev. *Special Functions & their Applications*.
- [9] D. S. Mataras, F. A. Koutelieris. *Programming in FORTRAN 90/95*.
Tziola publications Co. Thessaloniki
- [10] G.D. Bozis, I.D. Chatzedemetriou *Mechanics of Continuous Media*.
Tziola publications Co. Thessaloniki
- [11] N. K. Spyrou. *Stellar Evolution Principles*.
- [12] K. Kokkotas, N. Stergioulas. *Numerical Analysis*.
Lecture notes for the course “Numerical Analysis”.
- [13] N. Stergioulas. *Astrophysics-Cosmology*.
Lecture notes for the course “Computational Physics II”.
- [14] K. Daskalogiannis. *Special-Functions*.
Lecture notes for the course “Mathematical Methods of Physics II”

Websites:

- <http://www.nr.com/> *Numerical Recipes in Fortran 90*
- <http://lanl.arxiv.org/> *Physics e-Print archive mirror*